4-15-2014

Dynamics of Pyroclastic Density Currents: Conditions That Promote Substrate Erosion and Self-Channelization - Mount St Helens, Washington (USA)

Brittany D. Brand
Boise State University

Chelsea Mackaman-Lofland
University of Washington

Nicholas M. Pollock
University of Washington

Sylvana Bendaña
University of Washington

Blaine Dawson
Boise State University

See next page for additional authors

Authors
Brittany D. Brand, Chelsea Mackaman-Lofland, Nicholas M. Pollock, Sylvana Bendaña, Blaine Dawson, and Pamela Wichgers

Accepted Manuscript

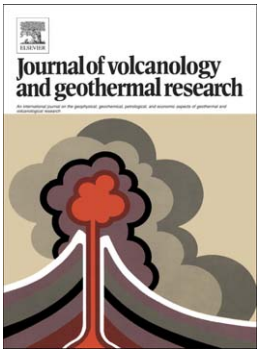

Dynamics of pyroclastic density currents: Conditions that promote substrate erosion and self-channelization - Mount St Helens, Washington (USA)

Brittany D. Brand, Chelsea Mackaman-Lofland, Nicholas M. Pollock, Sylvana Bendaña, Blaine Dawson, Pamela Wichgers

PII: S0377-0273(14)00021-3
DOI: doi: 10.1016/j.jvolgeores.2014.01.007
Reference: VOLGEO 5256

To appear in: *Journal of Volcanology and Geothermal Research*

Received date: 10 June 2013
Accepted date: 20 January 2014

Please cite this article as: Brand, Brittany D., Mackaman-Lofland, Chelsea, Pollock, Nicholas M., Bendaña, Sylvana, Dawson, Blaine, Wichgers, Pamela, Dynamics of pyroclastic density currents: Conditions that promote substrate erosion and self-channelization - Mount St Helens, Washington (USA), *Journal of Volcanology and Geothermal Research* (2014), doi: 10.1016/j.jvolgeores.2014.01.007

Manuscript Title: Dynamics of pyroclastic density currents: Conditions that promote substrate erosion and self-channelization - Mount St Helens, Washington (USA)

Corresponding Author: Brand, Brittany D.[1]
Corresponding Author Email: brittanybrand@boisestate.edu

List of Authors: Brittany D Brand[1,2], Chelsea Mackaman-Lofland[2], Nicholas M Pollock[2], Sylvana Bendaña[2], Blaine Dawson[1,2], Pamela Wichgers[2]

Author Affiliations: [1] Department of Geosciences, Boise State University, Boise, Idaho 83725-1535; [2] Department of Earth and Space Sciences, University of Washington, Seattle, WA 98195-1310

Abstract

The May 18th, 1980 eruption of Mount St. Helens (MSH) produced multiple pyroclastic density currents (PDCs), burying the area north of the volcano under 10s of meters of deposits. Detailed measurements of recently exposed strata from these PDCs provide substantial insight into the dynamics of concentrated currents including inferences on particle-particle interactions, current mobility due to sedimentation fluidization and internal pore pressure, particle support mechanisms, the influence of surface roughness and the conditions that promote substrate erosion and self-channelization. Four primary flow units are identified along the extensive drainage system north of the volcano. Each flow unit has intricate vertical and lateral facies changes and complex cross-cutting relationships away from source. Each flow unit is an accumulation from an unsteady but locally sustained PDC or an amalgamation of several PDC pulses. The PDCs associated with Units I and II likely occurred during the pre-climactic, waxing phase of the eruption. These currents flowed around and filled in the hummocky topography, leaving the massive to diffusely-stratified deposits of Units I and II. The deposits of both Units I and II are generally more massive in low lying areas and more stratified in areas of high surface roughness, suggesting that surface roughness enhanced basal shear stress within the flow boundary. Units III and IV are associated with the climactic phase of the eruption, which produced the most voluminous and wide-spread PDCs. Both flow units are characteristically massive and enriched in vent-derived lithic blocks. These currents flowed over and around the debris avalanche deposits, as evidenced by the erosion of blocks from the hummocks. Unit III is massive, poorly sorted, and shows little to no evidence of elutriation or segregation of lithics and pumice, suggesting a highly concentrated current where size-density segregation was suppressed. Unit IV shows similar depositional features but typically has a basal lithic-rich region, is variably

fines-depleted and contains pumice lobes, suggesting density segregation in a less concentrated current relative to Unit III. Deep, erosive channels cut by the Unit III current and thick lithic levee deposits within Unit IV occur in an area where debris avalanche relief is limited, suggesting self-channelization developed as a function of internal flow dynamics. An increase in the proportion and size of lithic blocks is found (1) downstream of debris avalanche hummocks, suggesting the PDCs were energetic enough to locally entrain accidental lithics from the hummocks and transport them tens of meters downstream, and (2) within large channels cut by later PDCs into earlier PDC deposits, suggesting self-channelization of the flows increased the carrying capacity of the subsequent channelized currents. Finally, the combination of thick, massive deposits with a high percentage of fine ash within Unit III and in the medial-distal depositional regions of Units II-IV suggests the PDCs developed and maintained a high internal pore pressure during transport and deposition. The most important include our ability to understand the role of internal pore pressure on current mobility, the influence of self-channelization on carrying capacity of the currents and the influence of surface roughness on substrate erosion. These observations have critical consequences for understanding the flow dynamics and hazard potential of PDCs.

1.0 Introduction

Pyroclastic density currents (PDCs), broadly considered one of the most dangerous volcanic hazards associated with explosive volcanism, are ground-hugging mixtures of hot gases and pyroclastic material driven by the force of gravity (Francis, 1993). PDCs can move at high velocities (>150 m/s), contain a wide range of initial particle sizes and concentrations, and are morphodynamic – they are highly unsteady and subject to rapid flow transformation due to changes in source conditions and interactions with the substrate (e.g., erosion, deposition, and topographic effects). Such changes lead to great vertical and lateral heterogeneity in both the current and the subsequent deposits. Identifying relationships between deposit characteristics and dynamic flow parameters, such as current velocity, concentration, particle support and depositional mechanisms, will provide a better fundamental understanding of how these parameters influence runout distance and the hazard potential of a current.

Observations of the May 18th, 1980 eruption at Mount St Helens (MSH), combined with recent exposures through the PDC deposits, provide an excellent opportunity to explore the relationships between current dynamics, depositional mechanisms and depositional features. Observations of plume height and ash dispersal constrain temporal variation in the mass flux throughout the eruption on May 18th (Figure 1 and Table 1; Carey et al., 1990). The afternoon PDCs that occurred on May 18th were documented and correlated with changes in eruptive intensity and behavior (Table 1; Criswell, 1987). Thirty years of erosion through the PDC deposits has produced some of the best vertical and lateral exposures through PDC deposits in the world.

The purpose of this research is to identify flow units, map changes in depositional features vertically, laterally and with distance from vent, and then use these relationships to

interpret the transport and depositional mechanisms within the depositional (basal) region of the currents produced during the afternoon of the May 18th eruption. The excellent exposures at MSH also allow us to explore the influence of surface roughness, substrate erosion and self-channelization as they are recorded in the PDC deposits, and to assess the influence of these factors on current mobility and run out distance. Our ultimate objective is to gain a better understanding of PDC dynamics from a field perspective and to provide well-constrained and data-supported interpretations and hypotheses that can be explored and tested via experimental and numerical techniques.

1.1 Eruption Chronology

The nine-hour MSH Plinian eruption that occurred on May 18th, 1980 is divided into the six eruptive phases (Table 1; after Criswell, 1987). The eruption initiated with an edifice collapse at 0832 PDT, immediately followed by a violent lateral blast resulting from decompression and rapid expansion of the over-pressurized magma beneath the bulging north flank (Phase 1; Criswell, 1987). Within a half hour the volcano produced a sustained, Plinian eruption column (Phase II; Criswell, 1987). Visual estimates of column height and subsequent measurements of ash distribution demonstrate that the magma mass flux slowly increased at the start and throughout Phase III of the eruption (Table 1: Criswell, 1987; Carey et al., 1990). As intensity increased throughout the early afternoon, many PDCs were generated due to column collapse (Phase III; Fig 1), the most voluminous of which were funneled down the northern breach in the volcano. The PDCs from this period are described as being generated by low, dense clouds that initially rose above the crater, but then collapsed through the northern breach resembling a "pot boiling over" (Rowley et al., 1981).

Phase IV represents the climactic phase of the May 18th eruption (Criswell, 1987). During this time the explosive intensity and mass flux were at their highest, likely as a function of conduit erosion and widening (Rowley et al., 1981), which resulted in more voluminous pyroclastic flows. It is notable that between 1215 and 1630, ~77% of the total erupted mass could be accounted for in the PDC and co-ignimbrite ash deposits, while only ~23% was derived from eruption column fall out (Carey et al., 1990). After the climactic phase eruptive activity waned fairly rapidly. Between 1715 and 1815 the mass flux increased and decreased several times, occasionally producing small-volume PDCs (Phase V; Criswell, 1987). The final phase (Phase IV; 1815 to May 19, 1980) was characterized by a low-energy ash plume with transient increases in intensity (Criswell, 1987).

While the blast deposits have been studied in great detail (e.g., Hoblitt et al., 1981; Moore and Sisson, 1981; Fisher, 1990; Druitt, 1992), few studies have been conducted on the thick stack of PDC deposits. Most notable is the study by Criswell (1987), who was able to separate major flow units and link them with the eruptive phases that occurred throughout the day. However, Criswell's study was completed in the mid-80's when much of the deposits were still buried. In the subsequent 30 years, deeply incised drainages have provided new, extensive exposures that contain important information about the currents that produced them, and allow for a more rigorous study of the deposits to take place.

1.2 Pumice Plain Morphology and Relief

The debris avalanche that triggered the eruption left a large, horseshoe-shaped breach on the north side of the volcano (Figure 2). The northwestern flank of the volcano, west of the breach, has two breaks in slope, one just at the base of the steep volcanic slope transitioning from 26º to 10º, and another a kilometer to the north where the slope transitions from 10º to 4º (Figure

2a). The 10º slope is composed of debris avalanche deposits (Kuntz et al., 1990). The northeast flank of the volcano to the east of the breach has only one break in slope from ~23º to 5-7º, which is located at the base of the steep flank (Figure 2a). This becomes important when we discuss influence of slope on PDC transport and depositional mechanisms in subsection *5.2.1 Influence of slope.*

The pumice plain extends ~4 km from the base of the volcano to Johnston ridge (Figure 2a). The pumice plain was buried beneath 10s to 100s of meters of debris avalanche and blast deposits during the first phase of the eruption. The areas shaded yellow in Figure 2 represent debris avalanche hummocks, hereafter referred to simply as hummocks; areas shaded purple represent pre-1980 obstacles across the pumice plain.

The most voluminous PDCs from the afternoon of the May 18th eruption were primarily funneled through the breach on the north side of the volcano (Table 1; Rowley et al., 1981). Deposition occurred along the flanks and more than 8 km north of the volcano across the pumice plain (Figure 2). PDCs deposited up to 32 m of pyroclastic deposits in the area around the hummocks. Note that hummocks are scattered throughout the northwestern portion of the pumice plain, but are limited in abundance and spatial distribution in the northeast side of the pumice plain. This is important as it allows for a direct comparison of PDCs deposited in areas of low surface roughness (sample locations in open circles; Figure 2b), and high surface roughness where hummocks were between 10-50 m tall (sample locations in filled black circles; Figure 2b).

2.0 Methods

Basic stratigraphic measurements were completed throughout the pumice plain (major drainages named in Figure 2b). Facies analysis descriptions of deposit characteristics and measurements of thickness and grain size distribution within individual flow units with distance

from source are completed. Grain sizes are reported in phi (ϕ) units; $\phi = -\log_2 d$, where d is the particle diameter in millimeters (Krumbein, 1934). Coarse fractions (-6 ϕ and -3 ϕ ; 64-8 mm) were sieved in the field while finer fractions were collected and sieved in the lab. Image analysis was performed on scaled photographs for samples with clasts < -6 ϕ (>10 cm). A MicroTrak laser grain size instrument was used for grain sizes >2 ϕ (<0.25 mm). Juvenile pumice, crustal xenoliths and accidental lithic components were counted for componentry down to -3 ϕ in the field. Select samples were chosen for componentry down to 4 ϕ (a binocular microscope was used for grain sizes >0 ϕ).

"Fines depleted" is loosely defined in the literature as deposits that contain a lower amount of fine ash than the surrounding PDC deposits (Branney and Kokelaar, 2002). Fines-depletion gives some insight into the ability of a current to elutriate fines during transport, which provides insight into the degree of fluidization of the current. To assess the degree of fines depletion in the MSH PDC deposits, we follow the methods of Walker (1983) and calculate the ratio of the weight percent of ash greater than 4 ϕ (finer than 62.5 µm; F2) to the weight percent of ash greater than 0 ϕ (finer than 1 mm; F1). Ash greater than 4 ϕ is the most susceptible to elutriation (Walker, 1983), so the ratio provides a relative measurement of the amount of ash that was elutriated. As you will see in the data below, the ratio of F2 to F1 varies widely within the MSH PDC deposits. The average F2/F1 ratio for all of the PDCs generated on the afternoon of May 18th, 1980 is 0.23 with a standard deviation of 0.13. Given the data spread for the flow units of the May 18th, 1980 eruption, we consider F2/F1 ratios $\leq$0.1 as "fines-depleted" deposits, F2/F1 ratios $\leq$0.15 as "fines-poor" deposits, and $\geq$0.32 as "fines-enriched" deposits.

3.0 Results

3.1 PDC Flow Unit Components

Each flow unit contains varying amounts of ash, crystals, pumice and lithics. Three types of pumice are found within the afternoon PDC deposits: (1) white pumice with 62.82-63.45% SiO_2 and densities between 0.73-0.83 g cm^{-3}; (2) gray pumice with 60.47-62.42% SiO_2 and densities between 1.08-1.37 g cm^{-3}; and (3) banded pumice with 62.12-63.26% SiO_2 and densities between 0.84-1.28 g cm^{-3} (Criswell, 1987). Pumice contains ~33% phenocrysts comprised of plagioclase (0.2-3 mm), orthopyroxene (0.5 mm), amphibole (<0.5 mm) and iron-titanium oxides (0.5-2 mm), within a matrix of glass and microlitic crystals (plagioclase, opaque minerals and rare orthopyroxene and amphibole; Kuntz et al., 1981). Lithic clasts are a mixture of basalt, basaltic andesite, andesite, dacite, and rhyodacite with a wide range of vesicularity and variable degrees of hydrothermal alteration (Criswell, 1988 and this study). Lower crustal xenoliths are rare but present.

3.2 Terminology

A lithofacies is a non-genetic term defined as a set of distinct characteristics, which can include a combination of grain size, sorting, fabric and stratification. Lithofacies can repeat innumerable times throughout a particular pyroclastic sequence. Common lithofacies include massive tuff breccia, massive lapilli tuff or stratified lapilli tuff (a full list of lithofacies and their abbreviations are provided in Table 2). A flow unit is defined here as a package of lithofacies bounded by evidence for a break in deposition, interpreted as the passage and termination of a current.

3.3 Flow units

Five flow units were identified along the drainages in the pumice plain. Flow contacts vary from distinct, with sharp boundaries with underlying deposits, to diffuse or gradational boundaries. Thus identification of the five flow units presented below was only possible through detailed stratigraphy and mapping across the pumice plain, which enabled us to characterize and trace the nature of the deposit contacts and record vertical and lateral facies variations with distance from source.

Figure 3 is a representative stratigraphic column illustrating the average thickness and bedding characteristics of the four most extensive flow units, Units I-IV (see Table 2 for lithofacies abbreviations; see Table 3 for unit thickness with distance from vent). Unit V is only exposed within 5.25 km of the vent (beginning of the D-drainage). A brief description and interpretation of each flow unit is presented in Table 4. General statistics for lithofacies within each flow unit with distance from source are provided in Figure 4.

Even though PDC deposits are not representative of the entire current, basic deposit descriptions and measurements are the key to unlocking PDC transport and depositional history within the depositional region of the current, and are the first step to understanding the dynamics of the overall current. As such the interpretations in this paper refer to the conditions within the depositional region of each current at the time of deposition, unless otherwise noted.

3.4 Changes with Distance from Source

This section of the paper describes and correlates depositional changes within and between outcrops with distance from source (Figure 2b), and interprets them in terms of changes in PDC dynamics as a function of vent conditions, inherent current variability, surface roughness and slope. We also explore the controls of topography on flow dynamics. Localized, highly

eroded deposits can be found within the crater and flanks of the volcano, such as the proximal bedded deposits and massive deposits within the upper part of the breach (Rowley et al., 1985; Beeson, 1987). However, these are only locally exposed and largely inaccessible. As such we focus on the well-exposed deposits that infill the pumice plain. For simplicity we assume the starting location of the PDCs is the center of the crater. Distances from source are based on the flow lines of Kuntz et al (1990) and our mapping of flow directions (Figure 2c; Table 3).

3.4.1 Units I and II - Medial

Unit I is first exposed at outcrop AD-1, 5.7 km from source. It is present as a fines-depleted dxsLT capped with a thin (<50 cm) layer of fine-grained, massive ash (Figure 5b, c and 6a). It is 2.6 m thick at this location, although the base is not exposed. Unit I has a sharp contact with Unit II. Unit II is characterized as a 2.2 to 3.6 m thick, fines-depleted, reverse-graded dsLT (Figure 6a). Coarse-grained, poorly-sorted lensP are common in both units. Unit II is locally capped by a 20-50 cm thick layer of fine-grained, massive ash (Figure 5b, c).

Unit II outcrops again ~0.6 km downstream at outcrop AD-2b (Figure 7) where it is >5 m thick, although the base is not exposed. The unit grades from a poorly- sorted mLT at the base to a weakly-stratified and better-sorted dsLT towards the top (upper 1-2 m). Unit II thickens and grades downstream into mLT. Numerous coarse-grained, very poorly-sorted lensP are present, most of which are concentrated in the weakly stratified region of the deposit (Figure 6b; 7b). These lensP are coarser than those found at AD-1. The lensP are asymmetric in nature, with thick downstream terminations and thin tails pinching out toward source. Some lensP tails grade upstream into long, thin concentrations of pumice. Unit II is again capped by a thin (>50 cm), massive ash tuff, which has a gradational or sharp contact with the overlying mLT_{bl} lithofacies of Unit III.

Both Units I and II thicken and grade into more massive deposit in the medial-distal reaches of the pumice plain (7-8 km from source). Unit I is up to 12 m thick at AD-3a-b, 7.09-7.17 km from source, although the base is not exposed (Figures 6c, d; 8). The bedding characteristics and lithic concentration within this unit varies widely over short spatial distances (10s of meters). At AD-3a, Unit I is a poorly-sorted, lithic-rich mLT_{bl}. The unit is consistently fines-depleted across the entire exposure, including both the mLT and lensP lithofacies (Figure 4, 6c). Toward the center of the exposure, nearly half-way between AD-3a and AD-3b, Unit I becomes more block-rich with 10-20% lithic blocks at the base. The blocks decrease towards the center of the unit to <1% lithic blocks, then again coarsens upward in the last 1.5 m to contain up to 25% within the last 0.3 lithic blocks (Figure 6c). Unit I grades further to the north (AD-3b) into a massive-to-weakly sLT with abundant lensP (Figures 6d and 8a, b). The first 6.5 m of the Unit I is pumice rich; the last 4.5 m is reversely-graded and contains a greater portion of coarse lapilli to fine block-sized lithics. Unit I is locally capped by a 40 cm thick massive layer of fine ash layer.

The contact between Units I and II at outcrop AD-3a-b is sharp and somewhat planar. Unit II can be broadly characterized as a dsLT, although it ranges from massive and locally fines-depleted to well-stratified and fines normal (Figure 8). Unit II is up to 7 m thick on the south side of the outcrop (AD-3a), and is weakly-stratified with reverse grading of coarse lithics (coarse lapilli and fine block). Fine lithic blocks are more common towards the top of the unit, but comprise only 1-5% of the deposit. The largest blocks are on average 6.8 to 15 cm in their longest dimension; the largest block, located ~2 m below the contact of Unit II and III on the south side of the exposure, is 0.56 x 1 m (Figure 8a, b).

Unit II becomes more distinctly stratified towards the north side of the outcrop (AD-3b; Figures 6d and 8a, b; 9c). Strata are denoted by horizons of coarser (medium to coarse lapilli) clasts. The basal 3-5 m of the Unit II deposits are lithic rich. The upper 2-3 m of Unit II contains a higher proportion of pumice lapilli which form laterally continuous horizons within the flow unit. The pumice and lithic lapilli are generally asymmetrical, with their longest axis parallel to the bedding horizon.

3.4.2 Units I and II - Distal

T-1 (7.1 km from vent), T-2 (7.16 km from vent), AD-4 (7.8 – 8 km from vent) and K-1 (8.38 km from vent) represent the distal-most exposures of the afternoon PDC deposits. The deposits in these distal regions are generally more diffusely-stratified and fines-enriched than more proximal deposits, and contain a markedly higher percentage of coarse lapilli lensP and fewer blocks than upstream outcrops.

The contact between the debris avalanche and the May 18th PDC deposits is exposed at the base of outcrop T-1 and AD-4b. The four flow units are likely present at all distal locations but difficult to distinguish due to the lack of obvious flow boundaries and general stratified appearance of the outcrop relative to the more proximal exposures. Units I and II are generally combined due to lack of a clear flow boundary.

In locations T-1 and T-2, Units I and II are 11-14 m thick (combined estimate), although the base of the Unit I is not exposed at T-2. The deposits grade laterally between mLT and dsLT over short distances (10s of meters; Figure 10d-g). The mLT contains many alternating, discontinuous lensP and pumice horizons (10s of centimeters thick) and mT layers (centimeters thick, which results in a diffuse stratification throughout the lower flow units. A thin, decimeter-scale fine ash layer is intermittently found ~9.5 m into the sequence. All deposits are relatively

fine-grained (in comparison to more proximal deposits), but like the proximal deposits they are poorly-sorted (Figure 4). The mLT approaches fines-enrichment with a F2/F1 value of 0.32 at location T-2; lensP are enriched in fines. The samples taken from T-1 are anomalously fines-enriched relative to all other samples in the pumice plain with F2/F1 values near 0.63.

AD-4 is located 7.8 – 8 km from vent, just west of a cluster of debris avalanche deposits (Figure 2b). Unit I is in contact with the underlying lateral blast deposit at location AD-4 (Figure 11a). The lateral blast is easily distinguished by the presence of prismatic-jointed cryptodome dacite and charred wood. Several lithic lenses containing crytpodome dacite are present 3-5 m above the flow contact. The contact between Units I and II is indistinguishable, but the thickness between the base of Unit I and the inferred contact with Unit III suggests that Unit II is present and shares the same depositional characteristics as Unit I, as described at T-1 and T-2. Units I and II consist of a fines-enriched mLT with some diffuse stratification due to interlayers of mT and lensP. Our best estimate based on the intermittent presence of a fine-grained ash layer, which likely correlates with the ash layer found between Units I and II more proximal to source, is that Unit I is ~9 m and Unit II is ~4 m thick.

3.4.3 Units I and II - Interpretation

The deposits of Units I and II exposed more proximal to source (e.g., AD-1, AD-2b) are thinner and typically more stratified than those exposed more distal to source (e.g., AD-3, AD-4). This suggests conditions in the depositional region of the PDCs ranged from a granular flow-boundary and a traction transport flow boundary (Branney and Kokelaar, 2002). Basal shear stresses were high enough to form distinct, albeit poorly-developed stratification. Turbulence may have locally been an important particle transport mechanism in Unit I as evidenced by the cross-stratification at AD-1. The fines-depleted deposits at AD-1 suggests elutriation was

efficient at this location in the basal region of both Units I and II PDCs (Wilson, 1980; Druitt, 1995).

Units I and II are clearly thickening and becoming more massive with distance from source. This suggests that the PDC that produced Units I and II bypassed more proximal regions to deposit the bulk of its sediment load in medial to distal areas in a retrogradational fashion (e.g., Figure 6.12E in Branney and Kokelaar, 2002). The variable diffuse stratified to massive nature of the deposits within both units suggests that conditions fluctuated between fluid-escape and granular flow-dominated flow boundaries. The well-stratified deposits of Unit II on the north side of the outcrop at AD-3b are likely a consequence of instabilities in the current that locally increased bed shear stress (Figure 9b, c), which is further supported by the recent work of Mackaman-Lofland (in review). The lack of well-stratified deposits in Unit II at this outcrop and in other locations around the pumice plain suggest such instabilities were of short duration and only occurred locally. The slight increase in fine blocks often observed in the middle of Unit I and toward the top of the Unit II likely represents an increase in the mass flux at the vent, which would supply larger clasts to the current and provide an increase in carrying capacity (Branney and Kokelaar, 1992).

LensP that are asymmetric with pronounced downstream terminations and diffuse tails are interpreted to represent exposure in the direction of flow (e.g., Ad-2b, Figure 7b; Pittari et al., 2005); lensP that are more symmetric and diffuse in two directions, or are discontinuous lenses that grade vertically and laterally into additional pumice lenses or mLT (Figure 9c – base of Unit I exposure) are interpreted to represent exposure perpendicular to flow. The lensP within Units I and II are more symmetric and diffuse laterally at locations AD-1 (Figure 5) and AD-3 (Figure 9c), suggesting deposition occurred into or oblique to the outcrops. LensP at AD-2b (Figure 7b)

are intermediate, with some pronounced downstream terminations and elongated tails and other lensP that are more symmetric, suggesting deposition from more than one flow direction.

The laterally continuous nature of the capping mT and enrichment of fines suggests deposition from a co-ignimbrite ash that settled after the current ceased. The Unit I mT is fairly well-preserved across AD-1 and AD-3, suggesting little erosion by the Unit II current. The mT capping Unit II is less laterally continuous and fines poor to fines normal, and as such is interpreted to have been deposited by the waning tail of a PDC. It is also possible that the lateral discontinuity of the mT capping Unit II is consequence of erosion by the Unit III PDC. Shearing and/or mixing of fine grained granular substrates by overpassing non-fluidized and fluidized currents has been produced experimentally (Rowley et al., 2011; Roche et al, 2013), and as such is interpreted to be responsible for the mixed appearance of the Unit II-III boundary where the mT is not preserved.

The PDCs traveled over or around debris avalanche hummocks in all distal areas, as evidenced by the preservation of deposits between and downstream from the hummocks (Figure 2b). The most extreme example is at T-1 where PDCs traveled over hummocks with 30-50 m of relief. The diffuse stratification that appears throughout the distal outcrops within all flow units is interpreted to be the result of a combination of increased basal shear stress due to interaction with upstream hummocks and unsteadiness in the current. Despite the diffuse stratification, the internally massive nature of the Units I and II deposits suggest rapid deposition from a concentrated current. However, the enrichment of fines suggests the upward flux of interstitial fluid was negligible in the distal reaches, and thus that fluidization may not have played a significant role in the concentrated, basal, depositional region of the current. The lack of distinct

flow contacts suggest mixing of the subsequent currents with the freshly deposited previous units.

Evidence for erosion of the substrate by the Unit I currents is largely absent except in the most distal region of AD-4b, where large blocks of cryptodome dacite are present above the basal contact with the lateral blast deposit (Figure 13a). These cryptodome dacites blocks must have been plucked from some unknown (but likely nearby) upstream location and transported 10s to potentially 100s of meters downstream.

3.4.4 Units III and IV – Proximal

The most proximal pumice plain exposures of PDC deposits from the afternoon of the May 18th eruption are exposed 4.8-5.2 km from source in the C-drainage (Figure 2). Outcrop C-1 is located 4.8 km from source in a tributary of the large drainage on the western side of the pumice plain (Location C-1, Figure 2c). The outcrop is cut parallel to flow direction, which was from south (right) to north (left) in Figure 12c. Only Unit IV is exposed at this location, although the base is not exposed. The base of the exposed Unit IV sequence at C-1 begins with a fines-depleted basal mlBr, which grades vertically and laterally into a fines-depleted dsLT to mLT (Figure 12a). Blocks range from 0.64 to 1.2 m in size, and are composed of accidental lithics including basalt, andesite, dacite and rhyodacite. Weak imbrication is observed; the long axes of the blocks are roughly parallel to the depositional surface. The block-rich region is 3.5 m at its thickest (the base is not exposed at this location) and is 23 m in length. The blocks decrease in size vertically and splay at an upward, 15º angle in the downstream direction before diffusing into a dsLT to mLT (Figure 12c). Immediately downstream from the block concentration is a diffuse, 15 m wavelength dune-like feature with amplitude of 2 m. The stoss side dips at 7° to the south (apparent dip) and contains a larger proportion of coarse lapilli to fine

block-sized lithics than does the finer-grained (lapilli and ash) lee side, which dips at 13.5° to the north (apparent dip; Figure 12c). Minor lensP with an average percent of fines are present in the upper 1.5 m of the mLT on the downstream (north) side of the outcrop.

Section C-2 is 5.2 km from source and exposes Unit III and Unit IV (Figure 2). Unit III is a mLT ranging from 3 to 8 m in thickness; the base is not exposed (Figure 12b, d-e). The grain size distribution is poorly-sorted and somewhat bimodal with an average amount of fines (Figure 4; Figure 12b). Lapilli and blocks finer than -2 ϕ consist of 29% pumice and 71% lithics. No pumice lenses are observed. Unit III is capped by a massive, 20-26 cm thick layer of fine ash that pinches in and out laterally (Figure 12b, d).

Unit IV is 1.9 to 6 m thick, which is thinner than at the more proximal outcrop C-1. The deposits are fines-depleted, lithic and pumice rich and poorly-sorted mLT to dsLT (Figure 12b). Subangular coarse lithic lapilli and fine blocks (18-27 cm in diameter) are scattered throughout the outcrop; however, the large blocks that are observed in this unit at the more proximal C-1 deposit are not found here. Pumice lenses are more abundant than upstream, grain-supported, and vary in morphology from (1) somewhat symmetrical, convex lenticular lenses 0.35-0.8 m thick that diffuse laterally in two directions (1.9-3.5 m in total length), (2) asymmetrical lenses with downstream termination up to 3 m long and 0.5 m thick that diffuse in the upstream direction over distance of 4.5 m into mLT. The deposits overlying and juxtaposed to the lensP include dsLT and dxsLT. Crude dune-like structures are often present in these surrounding lithofacies (Figure 12b, e). Unit IV is overlain by a thin (centimeters), reworked layer and the deposits of the June PDC.

3.4.5 Units III and IV – Medial

To compare the influence of surface roughness, the medial location deposits are described along two transects, one with *negligible* surface roughness (G, F) and one with *variable* surface roughness due to scattered hummocks throughout the depositional region (D, AD) (Figure 2b).

3.4.5.1 Units III and IV – Medial with *negligible* surface roughness (G, F)

Units III and IV are exposed in the G-drainage, and are capped by the June and July PDC deposits (Lipman, 1980; Figure 10a, b). Unit III is a mLT with no apparent grading; the base is not exposed. The contact between Units III and IV at Location G is diffuse and indistinct, here only inferred based on the block-rich horizon near the center of the outcrop, which we correlate to the lithic-block rich base observed upstream at D-4 (described in detail below). With this flow boundary distinction, the lowest section of Unit IV is a mLT_{bl} with the five largest blocks between 0.54-0.65 m in their longest dimension (Figure 10b). The long axes of the blocks are typically parallel to the bedding horizon. The mLT_{bl} grades into mLT devoid of bedding features except for faint, diffuse stratification directly above the block-rich region (Figure 10b).

Depositional features are similar downstream at location F, except that the mLT_{bl} of Unit IV thins and the blocks fine over this distance (largest blocks <10 cm; Figure 10). Pumice lenses within Unit IV are coarser-grained and larger than at more proximal locations. The deposits dip gently in the downstream (north) direction at ~4-5º, consistent with the dip of the paleo-topography.

3.4.5.2 Units III and IV – Medial with *variable* surface roughness (D-AD)

Units III and IV are exposed along the >260 m, west-to-east, continuous exposure at D-4 (~5.5 km from source), which is cut roughly perpendicular to flow (flow direction is into outcrop; Figure 13). The base of Unit III on the west side of the exposure is marked by 1.4-4.5 wide, arcuate features that extend into the underlying Unit II deposits to depths of 0.6 to 1.4 m (Figure 6b). These features are filled with block-supported lithic breccias with varying amounts of ash and lapilli matrix. The five largest clasts within the scours range from 15-73 cm, although most scours contain an average block size between 11 and15 cm. Lithics are generally concentrated from the center of the scour towards the west (left), and to the top of the arcuate form. The percent of matrix increases from <5% to ~20% from left to right, becoming more matrix-supported within each arcuate feature from west to east (left to right; Figure 13b).

The base of Unit III grades laterally towards the east into a gradational contact between Units II and III with no pronounced arcuate features (Figure 13a). The mlBr base of Unit III is 0.6 to 1.3 m thick, and is commonly reverse graded. Above the mlBr is a 3.2-4 m thick mLT with no grading.

Unit IV has a sharp contact with underlying Unit III. Deep, arcuate features like those found at the base of Unit III are absent or unexposed, but shallower, more subtle arcuate features are common (Figure 13a). The mlBr is ~1.2 m thick, appears grain-supported and shows normal grading on the west side of the outcrop. To the east (right) the lithic-rich base becomes thicker (increasing to a thickness of several meters), forms a convex lens, and shows diffuse grain fabric that follows the convex profile and splays at 15-20° degrees to the left (Figure 13c-f). A second convex lens of lithic breccia with crude fabric occurs just a few meters to the east (right), separated from the first by a wide trough of mLT (Figure 13c-f). The second convex lens is ~6

m across and ~2 m thick, and also displays grain fabric that follows the convex profile. The photograph in Figure 13d was taken from across the drainage, on the south side of the channel. An identical feature with convex lenses is present on the south side, and lines up with the north at an azimuth of N25ºW. We use this azimuth to determine the flow lines at this location (Figure 2c).

The breccia concentration at the base of Unit IV has a sharp transition into a finer-grained mLT. The mLT is thicker in the trough between the two convex lenses, but is thin overlying the convex lenses. Unit IV has a sharp contact with the June PDC deposit on the west side of the exposure and with the lahar deposit on the east side of the exposure (Figure 13a, c-e).

Outcrop AD-1a, the first outcrop past the C-D convergence (Figure 2b), is located ~120 m from the D-4 outcrop. The dominant flow direction is into (at a slightly oblique angle) the outcrop shown in Figure 5b. Interestingly, the prominent, lithic-rich base of both Units III and IV found at D-4 are not present at AD-1. Instead the contact of Units II and III is sharp where the massive ash capping Unit II is present, but gradational where the massive ash cap is not present (Figure 5c). Unit III is a 5-7 m thick, block-rich, poorly-sorted $mLT_{bl\text{-}f}$. The first ~3 m of Unit III displays reverse grading of lithic blocks. The largest 5 lithic blocks range from 40 – 70 cm in their longest dimension, distinctly coarser than found at the upstream location of C-2. The blocks have an apparent imbrication fabric and appear to splay at 13-17° to the north (Figure 5b, c). Also common are meter-scale convex lithic lenses (lenslBr) with strong fabric and stratification that mimic the convex shape of the lenslBr (Figure 5b, c). The lithic lenses, not observed in more proximal locations, occur toward the top of the unit and outline channel-like features, which are filled with finer-grained mLT (letters *a*, *b* and *c* in Figure 5c).

Unit IV is a massive, poorly-sorted, variably lithic block rich unit, 3.5-4 m in thickness. Reverse grading and fines-depletion are found within the lower 2.8 m, followed by normal grading with an average amount of fines toward the top of the unit (Figure 6a). Like Unit III, the lithic blocks of Unit IV are dispersed at AD-1 and distinctly coarser than found at the upstream location of C-2. The five largest blocks range from 21-36 cm in their longest dimension; the average grain size of blocks is ~20-25 cm. However, unlike Unit III, the lithic blocks lack fabric and do not accumulate as lenslBr (Figure 5b, c). No lensP are noted in this location. Unit IV is capped by a thin veneer of the June PDC deposit.

To the west and slightly downstream, but still along the AD-1 outcrop, the contacts between Units II-III and III-IV become indistinguishable (Figure 5d). The contact between Units I and II is fairly sharp and marked by lensP and the fine-ash cap. The rest of the 32 m high outcrop appears as a thick, mLT_{Bl} with variable grading.

Outcrop AD-2b, located ~5.8 km from source, exposes Units II-IV (Figure 2b). The deposits have an apparent dip ~ 6º to the south toward the volcano (Figure 7b). The deposits at this location in general are much more distinctly bedded than in the more proximal regions, and thin within the outcrop up dip, away from source (Figure 7b). The contact between Units II and III varies between sharp, gradational and erosive. The first 2.5-4.5 m of Unit III is characterized by poorly-sorted mLT_{bl} with 6-15% fine lithic blocks (Figure 6b and 7b). The largest five clasts (all lithics) range from 24-31 cm in their longest dimension. These blocks are outsized relative to the more proximal locations of the C-drainage and relative to outcrops G and F (Figure 2). The blocks are more consistent in size with those found just upstream at AD-1.

Unit III ranges from ungraded to a slight reverse grading at the base, followed by normal grading at the top and depleted in fine ash. The mLT_{bl} is capped by a finer-grained ds-mLT that

is ~1.1 m thick. The ds-mLT grades vertically into a *second* 3.7 m thick, fines-depleted mLT, also mapped as Unit III (Figure 7b). There are fewer blocks (3-8%) and the deposit is relatively better sorted in this upper mLT than below. Note this is the only location across the pumice plain where Unit III is fines-depleted.

The contact between Units III and IV is sharp and marked by thin layer of fine ash (thickness of 10-20 cm), although the ash layer is not persistent across the exposure. Unit IV is characterized as a 2.3 m thick, fines depleted mLT to dsLT with <1% fine blocks and minor lensP (Figures 6b and 7). This unit is also anomalously fines-depleted relative to nearby outcrops (e.g., AD-1, G, F; Figure 4).

Outcrop AD-3a-b is a 400 m long outcrop trending north-south, which exposes Units I-IV. Flow direction was roughly into the outcrop from the southwest direction (Figures 2c and 8). A small phreatic explosion crater is located on the south side of the outcrop (Figure 8a, b). The explosion crater is rimmed by a thin veneer of surge deposits generated by the phreatic explosion, which also extend over a few 10s of meter away from the rim, and is filled with a lahar deposit capped with wind-blown ash.

The contact between Units II and III varies from diffuse on the south side of the outcrop to sharp on the north side. The contact between Units III and IV are also indistinguishable on the south side of the outcrop, and as such the units are described together for location AD-3 except within the channel where they are distinct (described below). Blocks comprise 5-10% of the unit(s). They are mostly scattered through the first 3 m of the 5 m thick unit, but show some faint grain fabric and splay features (splay features extend upward to the north at roughly 12°). The five largest blocks range from 40 - 97 cm in their longest dimension; the average grain size of blocks is ~75 cm, larger than found in upstream locations (G, F, AD-1, D or C-drainages).

The blocks are primarily oriented with their longest axis parallel to the bedding horizon. Overall, the unit has normal grading of blocks. The upper 2-3 m of the outcrop is characterized as a mLT.

Towards the east side of the outcrop (location AD-3b) the contact between Units II and III becomes sharp and forms a distinct, broad, U-shaped feature that truncates Unit II and extends down into Unit I (Figure 8 and 9). The U-shaped feature contains Units III and IV, which extend toward the north side of the outcrop and are oriented with a dip towards the center of the feature (AD-3b; Figure 8 and 9). The first 2-3 m of Unit III (within the U-shaped feature) is a mLT, which transitions abruptly into a 0.3 to 1.8 m thick, lithic block-rich concentration that extends 60 m along the south side of the U-shaped feature towards the axis. The five largest blocks within the U-shaped feature, which are composed solely of lithics, range from 69-100 cm in their longest dimension; the average grain size of blocks is ~82 cm. These blocks are significantly outsized relative to upstream outcrops. Blocks are oriented such that their longest (apparent) axis is parallel to the bedding plane. Blocks are composed solely of lithics. The block-rich region abruptly grades into a normal graded, mLT with <2% fine blocks (Figure 6d, 9), which thins away from the center of the feature.

Unit IV overlies Unit III within the U-shaped feature, with a sharp and erosional contact between Units IV and Unit III. Unit IV is up to 3.5 m thick; however, the top may not be fully preserved. The base of Unit IV is distinguished by a 0.62 to 2.25 m thick concentrated zone of lithic blocks. The average block size at the base of the massive breccia ranges from 0.20-0.40 m, and fines upward to an average block size of 0.12-0.15 cm. The five largest blocks range from 70-95 cm in their longest dimension, again, outsized relative to upstream outcrops. Like the lithic breccia in Unit III, the blocks, composed solely of lithics, are oriented such that their longest

apparent axis is parallel to the bedding plane (Figure 9). The block-rich region shows normal grading and a slight reverse grading at the top of the concentration towards the center of the U-shaped feature. It is overlain by a mLT similar to the mLT below in Unit III (Figure 9). Outside of the U-shaped feature to the south (toward AD-3b), the block-rich concentrations of Units III and IV pinch out and transition into diffuse strata and pumice lenses that dip to the south (Figure 9).

3.4.6 Units III and IV – Distal

The deposits at T-1 (7.1 km from source) are located on the downstream side of a cluster of 30-50 m tall debris avalanche deposits (Figure 2b), indicating the May 18th PDCs fill in, around and over the hummocks to deposit on the downstream side (Figure 2c). Location T-2 (7.16 km from source) is also directly downstream from a smaller debris avalanche hummock, which is nearly completely buried by the May 18th PDCs. AD-4 is located 7.8 – 8 km from vent, just west of a cluster of debris avalanche deposits (Figure 2b).

Individual flow units are difficult to distinguish in distal outcrops due to the lack of obvious flow boundaries and general stratified appearance of the outcrop relative to the more proximal exposures. Flow boundaries of Units III and IV are generally identified by a variably present fines-rich massive ash layer, capped by a lithic-block rich horizon that extends across the outcrops and can be correlated with upstream exposures. Blocks are typically less than 10 cm in their longest dimension and discontinuous across the base of each flow unit.

In all distal locations Unit III varies from 3.5 m (AD-4) to 5 m (T-1 and T-2) thick; Unit IV varies from 2.5 m (AD-4) to7.5 m (T-1 and T-2) thick. In both units a discontinuous, block-rich horizon at the base grades normally into a dsLT to mLT with a semi-laterally continuous capping layer of fine ash (pinches and swells slightly; Figure 10d-g). The deposits are generally

fines-average to rarely fines-enriched except in location T-1 where all samples taken from Units I-III are anomalously fines-enriched relative to any other exposure in the pumice plain (F2/F1 = 0.55-0.65; Figure 4).

An anomalous, coarse-grained lenslBr is located on the most proximal side of the T-2 outcrop, just downstream from the debris avalanche hummock (Figure 10d, e). The lenslBr is ~2.5 m thick and ~12 m in length, thinning and abruptly pinching out downstream (Figure 15c). The lithic lens is poorly-sorted with an average grain size is -3.5 ϕ. The long axes of the five largest blocks from that lens range from 0.31-0.52 m. The blocks show no preferred orientation or fabric. They are far outsized in comparison with other blocks at this location, or blocks found in the more proximal G and F-drainages.

Similar to more proximal locations, no lensP are observed in Unit III. However, lensP in Unit IV are common, larger in size and coarser-grained than in more proximal locations (e.g., Figure 11c). At locations T-2, AD-4b and K-1 lensP are elongated along strike with the outcrop and often have a thick downstream termination with tails that thin up-strike along the outcrop. The lensP can be 10s of meters in length. They are often capped by 10-15 cm of fine ash that thins with the tail. The deposits above and around the lensP are well-stratified, grading vertically and laterally into mLT where lensP are not present.

3.4.7 Units III and IV – Proximal Interpretation

The massive, poorly-sorted nature of the proximal Unit III deposit, first exposed at location C-2, suggests particle deposition from a concentrated current with rapid deposition and low bed shear stress. The lack of fines depletion throughout the deposit suggests that sedimentation fluidization within the depositional region of the current was not sufficient to elutriate the fines from the lower flow boundary at this distance from source (Wilson, 1980;

Druitt, 1995). The fines-rich cap is interpreted as suspension sedimentation either from the waning tail of the current or as co-ignimbrite fall out after deposition of the PDC ceased. This is one of the only locations across the pumice plain where the Unit III co-ignimbrite ash is preserved across the pumice plain (Figure 12b, d, e).

Unit IV is first exposed at location C-1 (Figure 12c). From map view (Figure 2a), it is clear that there are no significant topographic obstacles between location C-1 and the break in slope of the volcano. Pollock (2013) determined that the type and proportion lithic clasts present in the C-1 deposits are statistically similar to those found in the fall deposits, indicating they were primarily vent derived rather than eroded from the steep flanks of the volcano.

The break in slope from ~25º to ~4º is located ~640 m upstream from C-1, and likely had some influence on the deposition of the basal breccia at this location. The blocks may have deposited here due to (1) decreasing current competence after the break in slope (Freundt and Schmincke, 1985), (2) a hydraulic jump, which are common near a break in slope (e.g., Garcia and Parker 1989; Macías et al., 1998), or (3) some irregularity in the paleo-surface, such as a depression beneath the block-rich region of the outcrop.

The basal mlBr grades vertically and laterally into dsLT and mLT. The breccia at the base of the sequence suggests deposition from a density-stratified PDC that segregated the dense blocks toward the base of the current (e.g., Valentine, 1987; Macías et al., 1998; Branney and Kokelaar, 2002). The massive, fines depleted nature of the breccia suggests deposition from a fluid-escape dominated flow-boundary. However, the weak fabric suggests some influence of flow-boundary shear stress and thus some influence of granular transport on the mlBr deposits (Branney and Kokelaar, 2002). The fines poor, massive nature of the surrounding mLT suggests that the mLT was deposited by a concentrated flow with rapid deposition and low boundary

shear stress. The fines-poor nature of the mLT suggests elutriation was efficient, and thus that sedimentation fluidization was an important particle support mechanism in the depositional region of the current.

The most interesting observation at this outcrop is the mlBr that splays downstream into the block-free, regressive dune-like feature (Figure 12c). We interpret that the rapid deposition of the blocks created downstream instabilities within the current. A sudden decrease in the bulk density would cause an acceleration in the current (e.g., Bursik and Woods, 1996), which could locally increase bed shear stress, resulting in the dune-like feature.

The block-rich base of Unit IV is no longer present downstream at C-2 (Figure 12b, d), suggesting the dense blocks deposited from the current prior to this location. The vertical and lateral gradation between mLT, dsLT, dxsLT and lensP in Unit IV suggest the deposits were left by the current which varied both spatially and temporally from a fluid-escape dominated flow boundary zone to a traction-dominated flow boundary zone. The fines-depleted nature of the Unit IV lithofacies suggests elutriation was still efficient in the depositional region of the current at this location as well (Wilson, 1980; Druitt, 1995). The lack of obvious interaction with topographic obstacles between the source and C-2 suggest that the observed fines-depletion was an inherent process of the current rather than a result of surface roughness, likely due to the upward displacement of gas as particles settled (i.e. sedimentation fluidization; Wilson, 1980; Druitt, 1995; Branney and Kokelaar, 2002).

3.4.8 Units III and IV – Medial Interpretation

3.4.8.1 Units III and IV – Medial with *negligible* surface roughness (G, F) Interpretation

The lithic blocks are interpreted to mark the flow boundary between Units III and IV due to the common occurrence of blocks at this boundary across the pumice plain, and due to the

consistency in thickness of both units with the more proximal exposures. The decrease in grain size, increase in sorting and the increase in the proportion of fines within Units III and IV between outcrops G-1 and F-1 reflect decreasing energy and carrying capacity as the PDCs spread across the shallow-sloping pumice plain (e.g., Allen and Cas, 1988). The lack of fabric and massive nature of both Units III and IV suggest deposition from a concentrated current with rapid sedimentation and low boundary shear stress; however, the increase of F2 fines suggests that sedimentation fluidization was less influential as a particle support mechanism at these outcrop locations. The weak fabric within the lithic block horizon suggests some component of basal shear stress occurred in the block-rich portion of the density stratified flow.

3.4.8.2 Units III and IV – Medial with *variable* surface roughness (G, F) Interpretation

Units III and IV are much more variable along the D-AD transect. The mlBr base of both Units III and IV at D-4 provide evidence for a strong, locally-developed density gradient where the basal region of the current transports the coarse, dense blocks and the upper portion of the current transports finer-grained material (Figure 13; e.g., Macías et al., 1998; Branney and Kokelaar, 2002). The lack of obvious topographic obstacles between the D-4 location and the break in slope of the volcano (Figure 2c) suggests that the blocks at the base of Units III and IV were derived from the vent and/or steep flanks of the volcano. Pollock (2013) determined that the lithic population is statistically consistent with a mixture of vent-derived lithic (compared to fall deposits) and Castle Creek Andesite, an older lithology exposed in the wall of the breach where the steep flanks meet the shallowly dipping pumice plain (Hausback, 2000). This suggests some degree of flank erosion occurred near break in slope.

The arcuate scours on the west side of the outcrop at the Unit II-III contact indicate the Unit III current locally eroded into the underlying Unit II deposits as well. These are interpreted

as nested scours, labeled *a-d* according to the observed cross-cutting relationships (*a* is the oldest; *d* is the youngest; Figure 13b), suggesting a current with alternating cycles of erosion and deposition. The preferential deposition of blocks on the left side of the scours indicates a flow direction slightly to oblique and to the left (N-NW).

The contact between Units III and Unit IV at D-4 appears depositional and non-erosive (Figure 13). The top of Unit III at this location produces (from what we can see on the outcrop scale) a smooth surface that the following PDC traverses. The lithic lenses within Unit IV are interpreted to be lithic levees. This is supported by the strong fabric and stratification that defines the interior of the levees (Figure 13e, f). The nature of the flat contact between Units III and IV and the lack of obvious topographic influence upstream from this location suggests that the levee depositional features at this location are a consequence of flow self-channelization, where the non-uniformity of a flow spreading across a low sloping fan develops zones of faster moving flow axes known as thalwegs (e.g., Imran et al., 1998; Branney and Kokelaar, 2002). Levees can form as the result of (1) building up of coarse material along the sides of a thalweg as lateral static zones along channel margins (Félix and Thomas, 2004) and/or (2) increased friction along the outside of the flow behind the flow head and rotation of the velocity vector from the downslope direction along the center of the thalweg to the transverse direction toward the channel margins (Mangeney et al., 2007).

Regardless of the mechanism of formation, the lithic levees suggest self-channelization within the PDC that produced Unit IV. Each strata within the levees represents a different time surface as the current flowed and the deposit aggraded (Figure 13F; after Branney and Kokelaar, 2002), which suggests deposition from a locally sustained but unsteady current. The thick, block-poor mLT fill between the levees and the thin mLT overlapping the levees suggests that these

lithofacies were deposited during the waning phase of the Unit IV PDC. The thinning of the mLT over the levees is evidence that the later flow overtopped the levees, and that the surface roughness and levee features affected and partially-channelized the waning phases of the current (Figure 13).

The Unit III and IV deposit characteristics change drastically between outcrops D-4 and AD-1 (Figure 5a). At AD-1, Unit III contains a high percent of lithic blocks relative to upstream D- and C-drainage locations. These blocks are larger and more dispersed than observed at nearby outcrop D-4. The flow lines, which represent the estimated path for Units III and IV only, indicate that the deposits at AD-1 were transported by the same current over a different flow path than those at D-4, likely converging near the junction of outcrops D-4 and AD-1. The Unit III PDC would have traveled (1) down the main breach into the pumice plain and directly into the D-4 location, skirting the hummocks to the west, and (2) down the steep northwestern fan of the volcano outside of the breach directly toward AD-1. The western portion of the current would have surmounted and/or traveled just to the west of the debris avalanche hummock upstream from AD-1. We interpret that the increase in the size and proportion of lithic blocks at AD-1 is due to higher current competency as a result of the greater slope of the northwest flank and the more direct flow path. It is also possible that some of the blocks were derived from the upstream debris avalanche hummock (Pollock and Brand, 2012; Pollock, 2013).

Block imbrication is pervasive in Unit III at AD-1, as illustrated with the dashed lines in Figure 5c. This imbrication suggests some influence of basal shear stress. However, the massive, poorly-sorted nature of the deposit suggests rapid deposition. Thus the flow boundary for the PDC responsible for the deposition of Unit III at AD-1 is interpreted to be a gradation

between granular flow and fluid-escape conditions; flow unsteadiness and transformation was likely due to the increased surface roughness upstream from this outcrop.

The accumulations of convex lenslBr, with strong fabric and stratification that mimic the shape of the lens, are interpreted to be a result of the onset of levee formation (Figure 5c). The levees here are poorly-developed relative to those at D-4, and as such may represent the beginning development of multiple thalwegs (e.g., Imran et al., 1988). The finer-grained, essentially block-free mLT that fills in between the lithic levees (labeled *a*, *b* and *c* in Figure 5c) is interpreted to be the result of deposition from the waning phase of the current.

There are strikingly fewer blocks in Unit IV at AD-1 than at D-4. This indicates the Unit IV current was less voluminous and did not produce a substantial current down the northwest flank, as did the Unit III current. In contrast, Unit IV at AD-1 was likely deposited by a concentrated current with rapid sedimentation and low basal shear stress with minor fluctuations toward a granular flow boundary, as evidenced by the predominantly massive nature and weak to non-existent fabric. The normal grading suggests deposition from a waning current. The range from fines-depleted to fines normal suggests the process of elutriation, likely due to sedimentation fluidization, continued to occur up to this distance from source. This marks the furthest lateral extent of obvious fines-depletion within Unit IV.

Many of the contacts between Units III and IV for outcrops AD-1 through AD-3 are indistinct or completely unrecognizable. In general, the diffuse or indistinct flow boundaries are interpreted to reflect variable erosion, shearing and/or mixing with the previous flow deposits (i.e., Calder et al., 2000; Rowley et al., 2011). The most striking example of completely erased flow boundaries occurs where AD-1 transitions from the east side of the outcrop, where flow contacts are somewhat recognizable, to a thick wall of mLT_{Bl} on the west side of the outcrop,

where no evidence for flow boundaries between Units II, III and IV are apparent (Figure 5d). We interpret that the lack of distinct flow boundaries is due to increased frictional forces at the bed due to the upstream break in slope from 10º to <5º (Figure 2a; Sulpizio and Dellino, 2008; Sulpizio et al., 2008). Downstream from the break in slope the depositional region of the current likely collapsed, resulting in rapid deposition and massive deposits (Kneller and Branney, 1995; Giordano, 1998; Branney and Kokelaar, 2002; Pittari et al., 2006; Sulpizio et al., 2008). The lack of flow boundaries is important to consider when studying PDC deposits with limited exposure because such a section could easily be misinterpreted as consequence of a single semi-sustained current rather than multiple currents with amalgamated flow contacts.

Many debris avalanche hummocks are exposed starting around the AD-1 drainage, and as such many more are likely buried north of AD-1 towards outcrop AD-2b. Thus the 6º (apparent) dip to the south and thinning of the deposits to the north at AD-2b reflects a change in slope from north dipping to south dipping of the surface topography, likely due to buried hummocks beneath the PDC deposits (Figure 7).

The most striking observation at AD-2b is the repeated section of Unit III. The first Unit III sequence is much coarser-grained than the second Unit III sequence. The flow lines in Figure 2c demonstrate that part of the PDC responsible for Unit III traveled down the steep northwestern flanks and had a more direct and shorter route toward outcrop AD-2b, whereas the portion of the current that traveled down the breach and curved to the west around outcrop D-4 had a longer travel distance to AD-2b. Like the interpretation for the increased block size at AD-1, this suggests that the portion of the current traveling down the steep flanks of the northwestern slope maintained higher energy and carrying capacity, resulting in coarser-grained deposits in the first section of Unit III. The shorter travel distance also indicates the northwestern-derived flow

would arrive before the portion of the flow that traveled through the breach, which accounts for the 'repeated' sequence of Unit III. The second Unit III sequence contains fewer blocks than the first, suggesting a current with lower carrying capacity at this location, possibly due to the longer flow path. The greater thickness of the second Unit III sequence suggests a larger portion of the current was directed down the breach relative to the portion of the current that traveled down the northwestern flank.

The fines-poor to fines-depleted nature of the Unit III mLT at AD-2b is unusual compared to the fines normal to fines enriched nature of Unit III at most other locations across the pumice plain. We interpret the lack of fines to be a consequence of increased elutriation efficiency due to air ingested and mixing as the flows collided. The stratified nature of the lapilli tuff capping the first Unit III sequence might reflect local instabilities and fluctuations in the current during or shortly after collision, or an increased and continued flux of the Unit III current through the crater breach. The fines-depleted nature of Unit IV suggests that flow collision may have occurred for the Unit IV PDC at this location as well. However, the absence of a repeated unit or changes in block size suggests this may have occurred to a lesser extent for the Unit IV current relative to that of the Unit III current.

AD-3 represents the medial-distal outlet of the currents that traveled through the breach and/or along the northwest flank. The flows turned toward the west, as evidenced by the flow direction indicators throughout the outcrops (e.g., levees, lensP orientations; Figure 2c). The Unit III PDC carved a large, wide channel into the Unit II deposits. The channel was subsequently filled with mlBr and mLT of Units III and IV. This is a clear example of self-channelization, where the current spreading across the pumice plain began to preferentially channelize and carve into the underlying substrate. Within the channel, the deposits begin with mLT, suggesting the

erosive current became depositional and began to fill the channel as the concentrated current continued to pass. The abrupt increase in blocks (mlBr) with no obvious break in deposition suggests an increase in mass flux and lithic material at the vent (e.g., Branney and Kokelaar, 2002). The outsized blocks relative to nearby Unit III and IV deposits suggests that channelization of Unit III resulted in a higher current competence. The sharp interface between the mlBr and overlying mLT in both Units III and IV suggests a sharp density gradient between the large, dense blocks that segregated to the base of the flow and the overlying mixture of gas, ash and (pumice, lithic) lapilli. The fabric observed in the mlBr, where the blocks are oriented such that their longest apparent axis is parallel to the bedding plane, suggest granular flow-boundary conditions; whereas the lack of fabric, poor sorting and fines normal nature of the mLT suggests deposition from a concentrated current with rapid sedimentation and low basal shear stress.

The outer channel deposits to the south contain elongated lensP and diffuse strata that dip 2-3º away from the axis of the channel (Figure 9). These are interpreted to be the result of the upper portion of a density stratified current that overtopped the margins of the channel, depositing the less dense (lensP) and finer-grained material. The diffuse contact between Units III and IV outside of the channel is interpreted to be the result of amalgamation (e.g., Calder et al., 2000; Rowley et al., 2011).

3.4.9 Units III and IV Distal Interpretation

The PDCs at T-1 traveled over the prominent distal hummocks (30-50 m of relief), as evidenced by the preservation of deposits between and downstream from the hummocks (Figure 10f-g). The PDCs of Units III and IV are interpreted to have spread across the shallowly-dipping pumice plain from the D-drainage, with some regions of the current traveling towards AD-4 and

some regions traveling north toward T-1 and T-2. PDCs at AD-4a and AD-4b flowed in and around some of the small hummocks on the southwest and west side of the debris avalanche cluster near AD-4a and AD-4b, as evidenced by minor filling in of the low ridges. However, the pronounced lensP downstream terminations with tails that thin toward source at AD-4b suggest this outcrop was cut parallel to flow direction flow, and thus that the primary flow direction was *around* the west side of the debris avalanche (Figure 2c). Similar to location AD-4, the pronounced downstream terminations of the lensP to the west with tails that thin toward the east suggest that outcrop K-1 was cut parallel to flow direction. As such, the deposits in the K-drainage are inferred to have wrapped around the east side of the debris avalanche cluster and traveled along the same orientation as the present Toutle river drainage.

The diffuse stratification that appears throughout the distal outcrops within all flow units is interpreted to be the result of a combination of increased basal shear stress due to interaction with upstream hummocks and inherent unsteadiness in the current. However, the internally massive characteristics of Units III and IV suggest rapid deposition from a concentrated current. The enrichment of fines suggests the upward flux of interstitial fluid was locally, and thus that fluidization may not have played a significant role in the concentrated, basal, depositional region of the currents distally. The lack of distinct flow contacts suggest mixing of the subsequent currents with the freshly deposited previous units.

Similar to other medial to distal locations, the lithic-rich horizons are interpreted to mark the basal contacts of Units III and IV. We recognize that the lithic-rich horizon at what we consider the Units II-III and III-IV contacts could represent an increase in mass flux at the vent within a given current. However, we interpret the lithic-rich horizon as marking the flow boundary due to the appearance of this layer at the base of Units III and IV across the pumice

plain, and due to the consistency in the thickness of both units with more proximal exposures. A similar gradation from lithic breccia to one-clast-thick, block-rich basal zones has been recognized elsewhere (e.g., Kos Plateau Tuff; Allen and Cas, 1998). The lack of a distinct flow boundary between the two units likely reflects erosion, shearing and or mixing with the underlying PDC deposits (Calder et al., 2000).

A lenslBr at the base of Unit III is located just downstream from an exposed hummock at outcrop T-2 (Figure 10d, e; 15c). The juxtaposition with the hummock, concentration and outsize nature of the blocks, and increase in the amount of hydrothermally altered material within the lens suggests the blocks were eroded from the upstream hummock (Pollock and Brand, 2012; Pollock, 2013). The position of the lenslBr at the base of the flow unit suggests erosion occurred with the passing of the current head. This supports the idea that underpressure at the head of the current is capable of producing a lift force along the substrate and entraining large blocks, as discussed in Roche et al. (2013). This is considered further in the discussion below.

In Unit IV, the increase in lensP thickness and length, increase in lensP average grain size and juxtaposition of lensP with lithic-rich mLT with distance from source suggests the pumice did not segregate and decouple from a more lithic rich basal region of the flow, as interpreted in Calder et al. (2000) and Pittari et al., (2005). Instead, in this case it is more likely that the lensP effectively segregated a proportion of the pumice into concentrated lenses, which traveled at the level of neutral buoyancy until the current's density decreased to less than that of the pumice concentrations, resulting in en masse deposition of the lensP (e.g., Druitt, 1995). This suggests laminar flow at least within the depositional system. Stratification juxtaposed to lensP is common but typically fades laterally into mLT, and as such is interpreted to be the result of

increased surface roughness, which disturbed the flow boundary and locally increased basal shear stress.

3.4.9 Pumice Rounding (comminution)

Rounding of pumice in PDC deposits reflects abrasion and production of comminuted ash during transport (e.g., Manga et al., 2011). Increasing the amount of comminution-ash in a PDC can result in an increase internal pore pressure, which has been shown to increase flow mobility and carrying capacity resulting in longer runout distances than PDC flows with less ash (e.g., Dufek and Manga, 2008; Roche, 2012). We used a 2-D image analysis technique described in Manga et al. (2011) where the roundness value of a pumice is calculated using $R = \frac{4\pi A}{P^2}$ (A is the cross sectional area and P is the perimeter of the pumice clast). For simplification only the outcrop data for Unit IV is presented although the results are consistent for all units analyzed (Dawson et al, 2011).

The frequency of roundness for 8-16 mm and 16-32 mm clasts is consistent across the extent of the pumice plain within Unit IV, as represented in Figure 14b. The 8-16 mm clasts appear to be slightly more rounded than the 16-32 mm values, though they are within 0.05 of the larger clasts and bulk unit values (Figure 14a). The pumice within the PDCs had reached maximum roundness *before* entering and depositing across the pumice plain. This is consistent with the results of Manga et al. (2011), who obtained the same results and suggest that most abrasion occurs in the energetic proximal regions of the currents as they descend the steep flanks of the volcano. However, at location T-1 (located directly downstream from a series of hummocks; Figure 2b), there is a decrease in roundness for the 8-16 mm grain size and the bimodal distribution for the 16-32 mm clasts.

We suggest that the sudden interaction of the PDCs with an up to 50 m tall assemblage of debris avalanche hummocks, the largest the PDCs interacted with across the pumice plain, likely caused a densification (increased concentration) within the basal region of the current. Densification would increase the potential for pumice breakage and production of ash due to collisional or frictional processes within the basal region of the current.

4.0 Discussion

The exposures throughout the pumice plain enabled us to map the major flow units and determine the influence and effect of substrate roughness on both small scale current conditions, such as transitions in localized flow boundary conditions and particle-particle interactions, and large scale current conditions, such as erosion of hummocks and scouring of earlier PDC deposits. Here we present a summary of these findings and discuss (1) probable correlation of each PDC unit with visual observations from the eruption, (2) the nature of each current as the PDCs filled in the pumice plain, including the role of fluidization as a particle transport mechanisms (3) the conditions that favor (and consequences of) erosion and self-channelization.

4.1 Correlation with eruptive events

The pumice plain and other areas north of the volcano were largely obscured and/or inaccessible throughout the eruption (Dr. Don Swanson, USGS, Personal Comm.). Despite this, several key observations allow the relative timing, duration and mass flux for each of the PDCs responsible for the five flow units to be constrained, which are critical input parameters for future modeling efforts.

The first major afternoon PDCs occurred during the pre-climactic, waxing phase of the eruption (1217-1500; Table 1). The currents "poured through the breach" northward through the crater and are infamously described as resembling a "pot boiling over" (Rowley et al., 1981;

description of D.A. Swanson of USGS, reported in Criswell, 1987). PDCs to the north began around 1220, increasing in volume by 1225, becoming "very intense and vigorous" by 1228, and were recorded as "continuously increasing in volume" at 1248 (USFS radio log May 18, 1980; Criswell, 1987). This description could be interpreted as a single, sustained PDC that varied in intensity over a minimum of 28 minutes, although it is not noted when the PDC ceased. PDCs flowed more episodically from 1330 to 1500, which suggests pulsating behavior and likely multiple PDCs. However, the duration of the current(s) and distance over which they traveled (i.e., whether or not they entered the pumice plain) was not possible to determine due to poor visibility north of the volcano. Smaller PDCs were noted to flow down the east, south and west flanks of the volcano during this time. PDC activity was noted to again increase between 1430 and 1550.

Unit I is related to deposition between 1220 to at least 1248, although the "increasing volume" noted at this time suggests the flow(s) were still increasing in vigor. It is unclear if a single, sustained PDC or multiple PDCs traveled through the breach, or when exactly the early ash flow PDC activity ceased. The thickness of Unit I could suggests deposition from a locally sustained PDC or an accumulation of multiple, unsteady PDCs with amalgamated contacts. 'Locally' sustained implies the depositional system of a current responds slower than fluctuations in the current, due to inherent unsteadiness or unsteadiness at the vent. We do not mean to imply truly steady flow conditions feeding the current or within the current. A co-ignimbrite ash column was noted to extend 4-7 km north of the crater at 1407 (USFS radio log; Criswell, 1987), which we correlate with the capping massive tuff of Unit I, further supporting the interpretation of deposition via a co-ignimbrite as fall. Thus the Unit I PDC flowed over a minimum of 28 minutes and maximum of 100 minutes.

Unit II is loosely correlated with the increase in activity between 1430 and 1550. This is primarily based on the evidence for a break in deposition between Units I and II (mT capping Unit I). It is again unclear if this phase of PDCs was locally sustained for a period of time or generated as PDC pulses from the vent; however, the thickness of the deposits suggests a somewhat sustained current or multiple, unsteady PDCs with amalgamated contacts.

The climactic phase of the eruption produced the most voluminous and wide-spread PDC(s). The increase in lithic blocks within the deposits of Units III and IV suggest significant vent-widening, which also correlates with the increase in mass flux during this time (Criswell, 1987; Carey et al., 1990). Observations reported in the May 18, 1980 USFS radio log (published in Criswell, 1987) vaguely describe "numerous, large" PDCs generated during the climactic phase, which engulfed the volcano. At 1501 a PDC was observed to reach Spirit Lake, at 1528 PDCs were again reported through the north breach. However, is it unclear if these were the same, sustained PDC or multiple PDCs (due to lack of visibility to the north). PDC activity to the north waned between 1605-1620, and "abated" at 1635 (Criswell, 1987). This suggests that the current was sustained and/or fluctuating from 1501 or 1528 to 1635. Meanwhile many smaller PDCs occurred on the east, south and west flanks of the volcano. The eruption began to wane around 1715. However, a short-lived increase in activity at 1745 produced "several" PDCs to the north, reaching Spirit Lake by 1747, and continuing until 1810. After this time PDC activity ceased and the eruption continued to wane.

Unit III is confidently associated with the climactic phase PDCs based on the distribution, thickness and increased lithic block content. This is the only flow unit which can be definitively related to a period in the eruptive sequence based on comparison of depositional features and observations of the eruption column during this time. It is unclear if Unit IV was also produced

during this time or was a consequence of the 1745 PDCs during the late ash flow phase. There is some evidence of a pause between these two flows (e.g., the rarely-preserved mT layer at C-2), which could be explained by an hour break in the flows; however, the development of lithic levees, which necessitate locally sustained flow, and the block-rich nature of the deposits could be argued to be depositional characteristics more consistent with the current(s) produced between 1500-1635. Regardless, the thickness of Units III and IV scour and fill features (Unit III) and development of lithic levees (Unit IV) suggest locally sustained flow. Real-time observations of the PDCs indicate that each of these two flow units may in fact preserve multiple, pulsating flows that are not recognized due to amalgamation of the flow contacts, as documented in the 1993 Lascar PDC deposits by Calder et al., (2000).

Flow Unit V, where exposed, has fewer lithic blocks than the underlying Units III and IV, a much higher percentage of pumice blocks (some more than 1 m in diameter), and is limited in distribution across the pumice plain. As such this is likely related to the final PDC(s) pulse, which occurred ~1810. The lack of deposits from Unit V near Spirit Lake rules out correlation with the 1745 PDC.

4.2 Fluidization and particle transport mechanisms through an evolving landscape

PDCs on the steep, proximal slopes of stratovolcanoes tend to be accumulative and non-depositional, effectively bypassing proximal regions (Giordano, 1998; Branney and Kokelaar, 2002; Brown and Branney, 2004; Pittari et al., 2006; Sulpizio et al., 2008). This explains the relatively thin PDC deposits found within the breach (Beeson, 1988) and complete lack of deposits found on the steep flanks of the volcano, although erosion likely also contributed to the lack of exposure. The first PDCs traversed the hummocky topography of the debris avalanche deposits and deposited the generally fines-poor stratified to diffusely-stratified Units I and II.

These units are thicker in the medial to distal of the pumice plain and thin toward source, suggesting retrogradational deposition (e.g., Branney and Kokelaar, 2002). The Unit I PDC was capable of plucking dense blocks from the substrate, as evidenced by the presence of cryptodome dacite within the Unit I deposits at distal location AD-4. However, both the Unit I and I deposits lack evidence of significant erosion of the hummocks. This suggests the early currents were of lower energy than the later Unit III and IV currents, and dominantly filled in between hummocks rather than traveling over (and eroding) them.

The pervasive fines-poor nature of Unit I (except for the capping mT, lensP and distal-most locations in the T-drainage) suggests a current that was conducive to sedimentation fluidization and elutriation of fines over the majority of deposition, even where depositing massive lithofacies, suggestive of concentrated flow conditions within the depositional system. This is likely due to the combination of a less concentrated current relative to Units II-IV, allowing sedimentation fluidization to occur within the depositional region of the current across the pumice plain, and the influence of surface roughness that likely existed between the larger hummocks. Both of these factors would promote non-uniformity within the PDC and elutriation of fine ash (cf. Giordano, 1998; Pittari et al., 2006; Sulpizio et al., 2008). Increased 'fluidization' due to interaction with surface water or vegetation can be ruled out since the debris avalanche buried the former landscape.

The Unit II deposits, which have evidence for non-uniformity (stratified deposits) but less evidence for fines elutriation beyond medial locations, suggest a current with slightly more concentrated conditions than the Unit I current. The Unit II current also likely experienced less surface roughness since the Unit I flows filled in the terrain and likely produced a relatively smoother surface that the Unit II PDC traveled across.

While the earlier currents were dominantly funneled through the breach and likely filled in and around topographic highs, the more voluminous PDCs of Units III and IV experienced the full impact of the high surface roughness and breaks in slope by traveling down the northwestern flank in addition to the north breach. The lack of fines depletion, lack of lensP, and the general distribution of lithic blocks throughout Unit III suggest that the depositional system of the current was at the high end of concentrated flow (40-65 vol% particles; Druitt, 1995). This resulted in a strong suppression of density segregation and elutriation across the entire pumice plain. However, the consistent deposit thickness and aerial extent of Unit III suggest a current with high mobility. Thus we interpret this current to have maintained a high internal pore pressure within the depositional region of the current across the entire outflow area, consistent with the experimental findings of Roche et al. (2004, 2008, 2010) and Roche (2012). Diffuse imbrication of blocks is noted in only some locations, such as at AD-1 and within the channel feature at AD-3, but generally fabric is weak to non-existent, suggesting granular flow conditions did not play a role (e.g., Cagnoli and Manga, 2005).

Within Unit IV, the presence of lithic blocks at the base at most locations, the abundance of lensP throughout the deposits, and general fines depletion at the proximal to medial regions suggests deposition from a current where size-density segregation and elutriation were efficient and a well-developed density gradient was established (e.g., Druitt, 1995). Like Unit III, increased surface roughness did not seem to significantly increase elutriation in these PDCs.

In addition to the observations of fines normal to enriched deposits in Unit III, Units II and IV clearly show evidence that, as the depositional regions of the currents compact with distance, sedimentation fluidization becomes negligible. Compaction of a fines-rich, gas-particulate current generates a high internal pore pressure. The experimental results of Roche et

al. (2010) demonstrate that, under these conditions, currents can maintain high pore pressure during most of the emplacement, supporting 70-100% of the weight of the particles. The high pore pressure also buffers particle interactions, resulting in an inertial, fluid-like behavior across much of their depositional region, and greatly increases the current's runout distance relative to non-fluidized currents (Roche et al., 2008, 2010; Roche, 2012). This is further supported by the relatively consistent deposit thickness of Units II-IV in the medial to distal reaches of the pumice plain. While pore pressure likely slowly diffused over the depositional area, there is no evidence, such as an increase in clast fabric, to suggest internal pore pressure completely diffused to transition the current into a granular flow. Scientists who visited MSH just after the 1980 eruption reported that the deposits were fluidized to the point of behaving like quicksand; several scientists reported repeatedly sinking hip-deep into the PDC deposits and being pulled out by colleagues (Dr. Richard Hoblitt, USGS, Personal Comm.). This further suggests the currents maintained some degree of internal pore pressure upon coming to rest.

4.3 Influence of Slope

While it seems that the most voluminous part of the Units III and IV currents were funneled through the breach, portions of the current also traveled down the slopes of the northwestern flank of the volcano, just west of the breach (USFS radio log May 18, 1980; Criswell, 1987). The steeper northwestern flank allowed the currents in that region to maintain momentum, energy and carrying capacity relative to the breach-funneled regions due to the greater slope and more direct flow path (Figure 2c). These currents reached the western fan of the pumice plain more quickly than the breach-funneled portions of the PDCs, depositing larger lithic clasts further distances from source (e.g., AD-1, AD-2b). The currents from the northwestern flank and breach wrapped around hummocks and collided at location AD-2b,

resulting in the variety of depositional features (Figure 7). This is the only location across the pumice plain where Unit III is found to be fines depleted (F2/F1 = 0.10-0.14), and suggests that PDC collision results in vigorous elutriation, likely due to mixing and ingestion of air at the interface of the collision.

A second clear example of the influence of slope occurs at the AD-1 outcrop, which is located at the second break in slope (10º to <5º) along the western side of the pumice plain and downstream from a large hummock (Figure 2a, b). The massive deposits with a lack of distinct flow boundaries at the western end of the AD-1 suggests that the upstream break in slope increased the pressure exerted during impact (Giordano and Dobran, 1994), increased basal friction (Sulpizio and Dellino, 2008; Sulpizio et al., 2008), and resulted in local erosion or shear-derived mixing (Rowley et al., 2011), erasing evidence of flow contacts. Flow deceleration and loss of capacity results in an increased boundary layer concentration and rapid sedimentation with negligible sorting (Kneller and Branney, 1995; Giordano, 1998), which explains the massive nature of the deposits.

4.4 Influence of Surface Roughness

In areas of low surface roughness, such as the G-F transect, the basal block rich region of Unit IV shows a general decrease in block size, in addition to a decrease in the median clast size within the mLT, and an increase in sorting, proportion of fine ash and abundance of lensP. This is expected for a current that loses energy, carrying capacity and the efficiency of elutriation as it flows and deflates away from source (e.g., Palladino and Valentine, 1995; Allen and Cas, 1998; Palladino and Simei, 2002). In contrast, Units III and IV within the AD-drainage show an increase in size and proportion of dense lithics with distance from source, which can be

explained by locally eroding lithic blocks from the debris avalanche and a higher carrying capacity for flows that became channelized (e.g., AD-3; Figures 8 and 9).

The influence of surface roughness is most obvious in the distal regions of the pumice plain where the Unit III and IV PDCs traveled and deposited over and around a concentration of hummocks (AD-4, T-1 and T-2; Figure 2b). The deposits in these distal areas are different in that they show diffuse to distinct stratification on the order of 10s of centimeters to meters. The layers are internally massive. The stratification is due to subtle changes in grain size throughout each flow unit, and is likely a result of increased shear stress as a function of higher surface roughness (Druitt, 1992; Giordano, 1998), flow unsteadiness and a decrease in suspended sediment load (Giordano, 1998; Figures 10d-f, 11).

The contacts between the hummocks and PDC deposits are also well exposed in the distal region of AD-4a drainage (Figure 15). Here the PDC deposits transition from dominantly massive upstream to cross-stratified as the currents travelled over the debris avalanche deposits (labeled DA in Figure 16). The mega-bedform shown in Figure 16c suggests that interaction with topography promoted turbulence induced traction transport, possibly enhanced by a decrease in suspended sediment load in the distal area (cf. Giordano, 1998).

The influence of surface roughness is also apparent on a much smaller scale with the juxtaposition of dsLT and dxsLT with lensP, which suggests that the deposition of lensP created small-scale surface roughness that locally increased basal shear stress (e.g., Unit IV at C-2, Figures 12d, e, and K-1, Figures 11b, c).These change in depositional regimes demonstrates the highly unsteady and variable nature of PDCs especially in the presence of surface roughness (Sulpizio et al., 2008).

Pumice is consistently found at maximum roundness within nearly all flow units at all distances across the depositional area, suggesting that abrasion and comminution occurred before the PDCs entered the pumice plain (e.g., Manga et al., 2010). This suggests that, even though the currents were likely concentrated and particle-particle collisions important, particle collisional energy was not sufficient to break the pumice because the pumice is not observed to be decrease in roundness. However, in tA *decrease* in pumice rounding is observed in only one location across the pumice plain – T-1. Just before depositing in the location the PDCs abruptly encountered a cluster of hummocks up to 50 m in height, the largest hummocks encountered by the PDCs (Figure 2b). Densification of the region near the flow boundary is interpreted to have increased as the PDC encountered the hummocks, also increasing pumice collisional energy to a point where breakage occurred. This is important as numerical models may be able to back out the bulk density conditions necessary to facilitate pumice breaking. This is also important as breakage of pumice would undoubtedly result in subsequent comminution, increasing the ash fraction and possible influencing runout distance or the ash available to loft into a co-ignimbrite plume.

4.5 Formation of Pumice Lenses

Pumice lenses (lensP) are interbedded with the stratified to massive, lithic rich tuff of Units I, II and IV. Therefore it is unlikely that they resulted from segregation of low density material that completely decouple from the lithic-rich portion of the current (e.g., Calder et al., 2000;Pittari et al., 2005). Density segregation and the formation of 'pumice rafts' apparently occurred within the flow as the low density pumice rose and accumulated at a level of neutral buoyancy in the flow (e.g., Druitt, 1995). The increase in abundance, size and grain size distribution of the lensP in the distal depositional regions indicates that pumice rafts developed

and grew through transport, and are interpreted to have been deposited when the current's depositional region reaches the density of the pumice accumulation (e.g., Druitt, 1995; Mackaman-Lofland, in review). The lensed nature of the lensP suggests they are deposited en masse (e.g., frozen) upon entering the depositional region of the current (e.g, Pittari et al, 2005).

4.6 Surface Erosion

The afternoon PDC deposits have a high percentage of accidental lithics, most of which have been previously interpreted as a result of erosion along the steep flank of the volcano (Rowley et al., 1981). However, comparison of the accidental lithic componentry between the fall and PDC deposits demonstrates that the majority of lithics were derived from vent erosion with only minor erosion along the steep flanks (Pollock et al, 2012; Pollock, 2013). However, erosion and plucking of lithics is obvious downstream from hummocks, where an increase in the concentration and size of dense lithics is routinely noted (Figure 15), indicating lithic blocks were plucked, carried and deposited 10s of meters downstream. These block lithics are not only outsized relative to surrounding PDC deposits where little to no evidence of interaction with hummocks is obvious, but in each case are also enriched in the lithologies found in the upstream hummock (Pollock et al, 2012; Pollock, 2013). Pollock (2013) also found an abrupt increase in the proportion of F2 fines in block-rich PDC facies found downstream from hummocks. The hummocks are enriched in fines relative to the PDC deposits. The increase in fines thus indicates matrix erosion was also significant (Pollock, 2013).

The increase in lithic clasts is most prominent at the flow contacts of Units III and IV, supporting recent experimental findings that an underpressure associated with the passing of the current head creates an upward force on the substrate, promoting "plucking" and erosion of the subsurface (e.g., Roche et al., 2013). However, hummock components are also found throughout

the entire thickness of a given flow unit downstream from source hummocks suggesting that basal shear stress, likely enhanced due to the high surface roughness, was also important in the process of erosion (Buesh, 1992; Sparks et al., 1997; Calder et al., 2000; Pittari et al., 2006). As the hummocks were progressively filled in, the percent of blocks derived from the hummocks approached zero, suggesting that erosion was enhanced by surface roughness and may also be supply limited (Pollock and Brand, 2012; Pollock, 2013).

4.7 Self-channelization

Self-channelization is evident from the lithic levees preserved within Unit IV at outcrop D-4 and the deep channel scour and fill in Unit III at outcrop AD-3b. Both examples occur in areas where significant debris avalanche hummock relief is limited, suggesting that self-channelization occurred independent of surface roughness. The levees of Unit IV (D-4) are deposited on the relatively flat surface of Unit III (from the outcrop perspective), representing a depositional expression (i.e., no obvious substrate erosion)and potentially the onset of flow self-channelization.

The large channel at AD-3b was carved by the passing of the Unit III PDC, providing an example of self-channelization dominated by erosion. The channel was subsequently filled by massive lapilli tuff and tuff breccias of Units III and IV. Pollock (2013) statistically determined that the lithic blocks filling the channel scour feature are primarily vent derived, suggesting the channelization likely began much closer to source and resulted in a higher carrying capacity of the currents.

Despite the occurrence of these two features in two different flow units, combining the presence of the lithic levees more proximal to source and channel scour and fill in more distal regions suggesting self-channelization may begin as a depositional occurrence but transition to

erosional downstream. Flows that develop thalweg zones are of higher flow capacity and competence and therefore promote erosion and scouring of the substrate. The accumulative nature is enhanced once self-channelization becomes well-established, resulting in continued and perhaps more substantial erosion. Once a channel develops, the channelized portion of the current that follows (1) maintains a higher capacity and competence, as evidenced by the outsized lithic blocks filling the AD-3b channel, (2) has an enhanced density gradient, as evidenced by the pronounced lithic breccia within each flow unit, and (3) has an increased runout distance, as predicted by numerical models (Bursik and Woods, 1996).

5.0 Conclusions

Column collapse and boil-over PDC behavior occurred during the afternoon of the May 18th, 1980 eruption during the waxing (early ash flow) phase, climactic phase, and waning (late ash flow) phase. Detailed measurements of exposed strata from these PDCs provide substantial insight into the dynamics of concentrated PDCs including inferences on particle-particle interactions, current mobility due to sedimentation fluidization and internal pore pressure, particle support mechanisms, the influence of surface roughness and the conditions that promote substrate erosion and self-channelization.

Debris avalanche hummocks scattered across the pumice plain north of the volcano provided meters to 10s of meters of vertical relief that the afternoon PDCs interacted with. The PDCs from the waxing phase traversed and filled in the hummocky topography, leaving the massive to diffusely-stratified deposits of Units I and II. The deposits of both Units I and II are thickest in the distal regions, suggesting retrogradational deposition. They are generally more massive in low lying areas and more stratified in areas of high surface roughness, suggesting that surface roughness enhanced basal shear stress within the flow boundary. Fines depletion is

pervasive in Unit I, suggesting that a combination of a lower particle concentration (relative to the later flows) and surface roughness between the hummocks promoted sedimentation fluidization and elutriation across the depositional area.

The climactic phase of the eruption produced the most voluminous and wide-spread PDCs (Units III and IV) which are characteristically massive and enriched in lithic blocks. These currents flowed over and around the debris avalanche deposits, as evidenced by the erosion of blocks from the hummocks. Unit III is massive, poorly-sorted, and shows little to no evidence of elutriation or segregation of lithics or pumice, suggesting a highly concentrated current with high internal pore pressure where size/density segregation was suppressed (Druitt, 1995; Druitt et al, 2007). The lack of pumice breakage indicates particle-particle interactions were buffered by a high internal pore pressure and thus a highly mobile, inertial flow behavior over much of the runout distance (cf. Roche et al., 2008; 2010; Roche, 2012). The lack of elutriation in Unit III and in the medial to distal deposits of Units II and IV suggest high particle concentration (e.g., Cerro Galan ignimbrite; Cas et al. 2011) and a sustained high internal pore pressure, resulting in a high current mobility and thus long runouts.

The increase in surface roughness before location T-1 changed the energy in the flow and increased basal shear stress and/or concentration, increasing the potential for pumice breakage and production of ash due to collisional or frictional processes within the boundary layer of the current. This caused pumice within the flow to break and re-round, increasing the ash content due to subsequent comminution. The breakage of pumice is important as numerical techniques may be able to constrain the conditions to promote pumice breakage (e.g., Dufek et al., 2012). Constraining the increased proportion of ash is important because ash content greatly influences the dynamics of a current (e.g., Dufek and Manga, 2008).

Deep, erosive channels cut by the Unit III current and thick lithic levee deposits within Unit IV occur in an area where debris avalanche relief is limited, suggesting self-channelization developed as a function of internal flow dynamics. The channel scour is filled with two lithic breccias from Units III and IV, both of which contain outsized blocks relative to surrounding, outer-channel deposits. This suggests that the carrying capacity and competence is increased for the channelized flows. The concentration of blocks and sharp transition into mLT also suggests a strong concentration gradient within the flow.

An increase in the size and proportion of lithics occurs downstream from debris avalanche hummocks within Units III and IV. Componentry analysis of the blocks demonstrates that many were eroded from the debris avalanche deposits (Pollock and Brand, 2012; Pollock, 2013). However, as the hummocks were progressively filled in, the percent of blocks derived from the hummocks approached zero, suggesting that erosion was enhanced by surface roughness and may also be supply limited (Pollock and Brand, 2012; Pollock, 2013).

The most important findings from this study include our ability to understand the influence of self-channelization on the carrying capacity of the currents and to understand the influence of surface roughness on substrate erosion. These observations have critical consequences for understanding the flow dynamics and hazard potential of PDCs. As with all research efforts, this study leaves us with more questions than we began with. We propose further exploration of the following topics through experimental and computational modeling investigations:

- It is unclear to what degree surface roughness influences fluidization and elutriation. Surface roughness is interpreted to have enhanced elutriation in Unit I, as suggested by the general fines depletion, but this had little to no effect on the later, more voluminous

currents that fully interacted with the debris avalanche deposits. Thus the influence of surface roughness on fluidization and elutriation remains poorly constrained.

- Flow convergences seem to enhance elutriation, likely due to mixing and ingestion of air. However, it is unclear exactly what happens when flows converge, how much ash is elutriated and available for transport into the atmosphere, and how this interaction influences downstream dynamics.
- There is good field and experimental evidence for the role of internal pore pressure and pore pressure diffusion in controlling the mobility of ash-rich PDCs. There is also evidence that some pore pressure is maintained during and after deposition. However, the mechanism for the onset of deposition in a fines-rich current with high internal pore pressure is poorly constrained (cf. Roche, 2012).
- Densification of the boundary layer upstream from obstacles, in some cases, leads to breakage of the pumice. It would be interesting to model the conditions necessary within the basal, depositional region of the current for this to occur as this may be a way to constrain bulk density near the flow boundary. This would also help constrain how much ash is produced via comminution, which can increase internal pore pressures and/or be available for escape into the atmosphere.
- What are the conditions that promote self-channelization and how does self-channelization evolve over time?
- What conditions favor erosion of the substrate in (locally) sustained currents long after the head of the current passes; how does erosion of the substrate (bulking of the flow, e.g, Calder et al., 2000) influence downstream dynamics (Pollock and Brand, 2012; Pollock, 2013)?

6.0 Acknowledgements

Funding for this work was provided through a National Science Foundation grant (NSF-EAR 0948588). The authors would like to thank Drs. Sharon Allen and Benjamin Andrews for their thorough and thoughtful reviews of our manuscript.

Allen, S. R., Cas, R. A. F., 1998. Lateral variations within coarse coignimbrite lithic breccias of the Kos Plateau Tuff, Greece. Bull. Volcanol. 59, 356-377.

Allen, J. R. L., 1985. Principles of Physical Sedimentology. Chapman and Hall, London.

Andrews, B.J., Gardner, J.E., 2009. Turbulent dynamics of the 18 May 1980 Mount St. Helens eruption column. Geology 37, 895-898.

Beeson, D.L. 1988. Proximal Flank Facies of the May 18, 1980 Ignimbrite: Mount St Helens. Washington. M.S. Thesis, University of Texas at Arlington.

Bendana, S., Brand, B.D., Self., S., Dufek., J., 2012. Effects of slope on the dynamics of dilute pyroclastic density currents from May 18th, 1980 Mt. St. Helens eruption. American Geophysical Union Annual Meeting. Abstract V41B-2778.

Brand B.D., Clarke, A.B., 2012. An Energetic Basaltic Phreatomagmatic Eruption at the Table Rock Complex in South-central Oregon (USA): Using deposit characteristics to constrain surge dynamics. J. Volcanol. Geotherm. Res. 243–244, 81–90.

Branney, M.J., Kokelaar P., 2002., Pyroclastic density currents and the sedimentation of ignimbrites. Memoir - Geological Society of London 27, 143

Branney, M. J., Kokelaar, B. P., 1992. A reappraisal of ignimbrite emplacement: progressive aggradation and changes from particulate to non-particulate flow during emplacement of high-grade ignimbrite. Bull. Volcanol., 54,504-520.

Brown, R.J, Branney, M.J., 2004. Bypassing and diachronous deposition from density currents: Evidence from a giant regressive bed form in the Poris ignimbrite, Tenerife, Canary Islands. Geology. 32, 445-448.

Buesch, D.C., 1992. Incorporation and redistribution of locally derived lithic fragments within a pyroclastic flow. Geol. Soc. Am. Bull. 104, 1193-1207.

Bursik, M. I., Woods, A.W., 1996. The dynamics and thermodynamics of large ash flows. Bull. Volcanol. 58, 175-193.

Calder, E. S., Sparks, R.S.J., Gardeweg, M.C., 2000. Erosion, transport and segregation of pumice and lithic clasts in pyroclastic flows inferred from ignimbrite at Lascar Volcano, Chile. J. Volcanol. Geotherm. Res. 104, 201-235.

Campbell, C.S., 1990. Rapid granular flows. Annual Review of Fluid Mechanics, 22, 57-92.
Carey, S., Sigurdsson, H., Gardner, J.E., and Criswell, W., 1990. Variations in column height and magma discharge during the May 18, 1980 eruption of Mount St. Helens. J. Volcanol. Geotherm. Res. 43, 99-112.

Crandall, D.R., Mullineaux, D.R., 1973. Pine Creek Volcanic Assemblage at Mount St Helens, Washington. Geological Survey Bulletin 1383-A:A6-A7.

Crandell, D.R., 1987. Deposits of pre-1980 pyroclastic flows and lahars from Mount St. Helens volcano, Washington: Lithology and stratigraphy of unconsolidated deposits, other than air-fall tephra, formed by eruptions during the past 40,000 years. In: Volcanic ash, tuff, etc.; Lahars; Geology; Washington (State); Saint Helens, Mount, vii, 91 p. U.S. G.P.O. (Washington and Denver, CO)

Criswell, C.W., 1987. Chronology and pyroclastic stratigraphy of the May 18, 1980 Eruption of Mount St. Helens, Washington. J. Geophys. Res. 92, 10237-10266.

Crowe, B.M., Fisher, R.V., 1973. Sedimentary structures in base-surge deposits with special reference to cross-bedding, Ubehebe Craters, Death Valley, California. Geol. Soc. Am. Bull. 84, 663-682.

Dawson, B., Brand., B.D., Dufek, J., 2011. Clast comminution during pyroclastic density current transport: Mt St Helens. Abstract : V51F-2575 presented at 2011 Fall Meeting, AGU, San Francisco, Calif., 5-9 Dec.

Druitt, T. H., Avard,G., Bruni, G., Lettieri, P., Maez, F., 2007. Gas retention in fine-grained pyroclastic flow materials at high temperatures, Bull. Volcanol. 69, 881-901.

Druitt, T. H., 1992. Emplacement of the 18 May 1980 lateral blast deposit ENE of Mount St. Helens, Washington. Bull. Volcanol 54, 554-572.

Druitt, T. H., 1995. Settling behavior of concentrated dispersions and some volcanological applications. J. Volcanol. Geotherm. Res. 65, 27-39.

Dufek, J., Manga, M., 2008. The in-situ production of ash in pyroclastic flows, J. Geophys. Res., 113, B09207. DOI:10.1029/2007JB005555.

Dufek, J. Manga, M., Patel, A., 2012. Granular disruption during explosive volcanic eruptions. Nat. Geosci. 5, 561-564. DOI: 10.1038/NGEO1524.

Félix, G., Thomas, N. 2004. Relation between dry granular flow regimes and morphology of deposits: formation of levees in pyroclastic deposits, Earth Planet. Sci. Lett. 221, 197-213.

Fisher, R.V., 1990. Transport and deposition of a pyroclastic surge across an area of high relief: The 18 May 1980 eruption of Mount St. Helens, Washington: Geol. Soc. Am. Bull. 102, 1038-1054.

Francis, P., 1993. Volcanoes – A planetary perspective. Oxford University Press Inc., New York.Freundt and Schmincke, 1985

Garcia, M. H., Parker, G., 1989. Experiments on hydraulic jumps in turbidity currents near a canyon-fan transition. Science. 245, 393-396.

Hoblitt R.P., Miller, D., Vallance, J.W., 1981. Origin and stratigraphy of the deposit produced by the May 18 directed blast. In: Lipman PW, Mullineaux DR (eds). The 1980 eruptions of Mount St. Helens, Washington. U.S. Geol. Surv. Prof. Paper. 1250, 401–419

Giordano, G., 1998. Facies characteristics and magma-water interaction of the White Trachytic Tuffs (Roccamonfina Volcano, southern Italy). Bull. Volcanol. 60, 10-26.

Giordano, G., Dobran, F., 1994. Computer simulation of the Tuscolano Artemisio's second pyroclastic flow unit Alban Hills Latium, Italy.. J. Volcanol. Geotherm. Res. 61, 69–94.Hiscott, R.N., 1994. Traction-carpet stratification in turbidites - fact or fiction? J. Sediment. Res. Section A. 64, 204-208.

Imran, J., Parker, G., Katopodes, N. 1998. A numerical model of channel inception on submarine fans, J. Geophys. Res. 103, 1219-1238.

Jessop, D.E., Kelfoun, K. Labazuy, P. Mangeney, A., Roche, O., Tilliere, J.-L., Trouillete, M., Thibaulte, G., 2012. LiDAR derived morphology of the 1993 Lascar pyroclastic flow deposits, and implication for flow dynamics and rheology. J. Volcanol. Geotherm. Res. 245-246, 81-97.

Kneller, B.C., Branney, M.J., 1995. Sustained high-density turbidity currents and the deposition of thick massive sands. Sedimentology, 42, 607-616.

Krumbein, W.C., 1934. Size Frequency Distributions of Sediments and the Normal Phi Curve. J. Sediment. Res. 8, 84-90.

Kuntz, M.A., Rowley, P.D., MacLeod, N.S., 1990. Geologic map of pyroclastic flow and related depostis of the 1980 eruptions of Mount St. Helens, Washington: U.S. Geological Survey Miscellaneous Investigations Map I-1950, 1:12,000.

Kuntz, M.A., Rowley, P.D., MacLeod, N.S., Reynolds, R.L., McBroome, L.A, Kaplan, A.M. Lidke, D.J., 1981. Petrography and particle size distribution of pyroclastic flow, ash-cloud and surge deposits, in Lipman, P.W., and Mullineaux, D.R., eds, The 1980 eruption of Mount St. Helens: U.S. Geological Survey Professional Paper. 1250, 525-539.

Lipman P.W., Moore J.G., Swanson D.A., 1981. Bulging of the north flank before the May 18 eruption - geodetic data. In: Lipman PW, Mullineaux DR, (eds). The 1980 eruptions of Mount St. Helens, Washington. U.S. Geol. Surv. Prof. Paper. 1250, 143–155

Lowe, D.R., 1982. Sediment gravity flows: II. Depositional models with special reference to the deposits of high-density turbidity currents. J. Sediment. Petrol. 52, 279-298.

Macias, J. L., Espindola, J. M., Bursik, M., Sheridan, M. F., 1998. Development of lithic-breccias in the 1982 pyroclastic flow deposits of El Chichon Volcano, Mexico. J. Volcanol. Geotherm. Res. 83, 173-196.

Mackaman-Lofland et al., in review. Sequential fragmentation / transport theory, pyroclast size-density relationships, and the emplacement dynamics of pyroclastic density currents – A case study on the Mt. St. Helens (USA) 1980 eruption. J. Volcanol. Geotherm. Res.

Mackaman-Lofland, C., Brand., B.D., Taddeucci, J., 2012. Particle size-density relationships in pyroclastic deposits: using component subpopulations to elucidate depositional conditions. Abstract V41B-2781 presented at 2010 Fall Meeting, AGU, San Francisco, Calif., 3-7 Dec.

Manga, M., Patel, A., Dufek, J. 2011. Rounding of pumice clasts during transport: field measurements and laboratory studies. Bull. Volcanol. 73, 321-333. DOI 10.1007/s00445-010-0411-6.

Mangeney, A., Bouchut, F., Thomas, N., Vilotte, J.P., Bristeau, M.O., 2007. Numerical modeling of self-channeling granular flows and of their levee-channel deposits, J. Geophys. Res., 112, F02017.

Middelton, G.V., Southard, J.B., 1984. Mechanics of Sediment Movement. Short Course Notes: 3. Society of Economic Paleontologists and Mineralogists, Tulsa.

Middleton, G.V., 1967. Experiments on density and turbidity currents III. Deposition of sediment. Can. J. Earth Sci., 4, 474-505.

Moore, J.G., Sisson, T.W., 1981. Deposits and effects of the May 18 pyroclastic surge. In: Lipman PW, Mullineaux DR, (eds). The 1980 eruptions of Mount St. Helens, Washington. U.S. Geol. Surv. Prof. Paper. 1250, 421–438.

Mullineaux, D.R., 1986. Summary of pre-1980 tephra-fall deposits erupted from Mount St. Helens, Washignton State, USA. Bull. Volcanol. 48, 17-26.

Palladino, D.M., Valentine, G.A., 1995. Coarse-tail vertical and lateral grading in pyroclastic flow deposits of the Latera Volcanic Complex (Vulsini, Central Italy): origin and implications for flow dynamics. J. Volcanol. Geotherm. Res. 69, 343-364.

Palladino, D.M., Simei, S., 2005. Eruptive dynamics and cladera collapse during the Onano eruption, Vulsini, Italy. Bull. Volcanol. 67, 426-440.

Pollock, N., Brand, B.D., 2012. Investigation into the erosive capacity of pyroclastic density currents at Mount Saint Helens, Washington (USA). Abstract : V54C-01 presented at 2010 Fall Meeting, AGU, San Francisco, Calif., 3-7 Dec.

Pollock, N., 2013. Field evidence for substrate entrainment by pyroclastic density currents and its effect on downstream dynamics at Mount St Helens, Washington (USA). M.S. Thesis, University of Washington.

Pittari, A., Cas, R.A.F., Martí, J., 2005. The occurrence and origin of prominent massive, pumice-rich ignimbrite lobes within the Late Pleistocene Abrigo Ignimbrite, Tenerife, Canary Islands. J. Volcanol. Geotherm.Res.139, 271-293.

Pittari, A., Cas, R.A.F., Edgar, C.J., Nichols, H.J., Wolff, J.A., Martí, J., 2006. The influence of palaeotopography on facies architecture and pyroclastic flow processes of a lithic-rich ignimbrite in a high gradient setting: the Abrigo Ignimbrite, Tenerife, Canary Islands. J. Volcanol. Geotherm. Res. 152, 273–315.

Pollock, N., Brand, B.D., 2012. Investigation into the erosive capacity of pyroclastic density currents at Mount Saint Helens, Washington (USA). American Geophysical Union Annual Meeting. Abstract V54C-01.

Roche, O., Gilbertson, M. A., Phillips, J. C., Sparks, R. S. J., 2004. Experimental study of gas-fluidized granular flows with implications for pyroclastic flows emplacement, J. Geophys. Res., 109, B10201, doi:10.1029/2003JB002916.

Roche, O., Montserrat, S., Niño, Y., Tamburrino, A., 2008. Experimental observations of water-like behavior of initially fluidized, dam break granular flows and their relevance for the propagation of ash-rich pyroclastic flows, J. Geophys. Res. 113, B12203. DOI:10.1029/2008JB005664.

Roche, O., Montserrat, S., Niño, Y., Tamburrino, A., 2010. Pore fluid pressure and internal kinematics of gravitational laboratory air-particle flows: Insights into the emplacement dynamics of pyroclastic flows . J. Geophys. Res.. 115, B09206. DOI:10.1029/2009JB007133.

Roche, O., 2012. Depositional processes and gas pore pressure in pyroclastic flows: an experimental perspective. Bull Volcanol 74, 1807-1820.

Roche, O., Niño, A. Mangeney, B. Brand, N. Pollock, G.A. Valentine., 2013. Dynamic pore pressure variations induce substrate erosion by pyroclastic flows. Geology. 41, 1107–1110.

Rosenbaum, J.G., Waitt, , R.B., Jr., 1981. Summary of eyewitness accounts of the May 18 eruption. U.S. Geol. Surv. Prof. Pap. 250, 53-68.

Rosenfeld, C.L., 1980. Observations on the Mount St. Helens eruption. Am. Sci. 68, 494-509.

Rowley, P. D., Kuntz, M. A. & Macleod, N. S. 1981. Pyroclastic flow deposits. In: Lipman, P. W. & Mullineaux, D. R. (eds) The 1980 Eruptions of Mount St Helens, Washington. US Geological Survey, Professional Papers, 1250, 489-512.

Rowley, P. D., Macleod, N. S., Kuntz, M. A., Kaplan, A. M., 1985. Proximal bedded deposits related to pyroclastic flows of May 18, 1980, Mount St Helens, Washington. Geol. Soc. Am. Bull. 96, 1373-1383.

Rowley, P., Kokelaar, P., Menzies, M., Waltham, D., 2011. Shear-derived mixing in dense granular flow. J. Sediment. Res. 81, 874-884.

Selim, M. S., Kothari, A. C. & Turian, R. M., 1983. Sedimentation of multisized particles in concentrated suspensions. American Institute of Chemical Engineers Journal. 29, 1029-1038.

Smith, R.L., 1960. Ash Flows: Geol Soc America Bull 71, 795-842.

Sohn, Y.K., Chough, S.K., 1989. Depositional processes of the Suwolbong tuff ring, Cheju Island (Korea). Sediment. 36, 837-855.

Sparks, R. S. J., 1976. Grain size variations in ignimbrites and implications for the transport of pyroclastic flows. Sedimentology. 23, 147-188.

Sparks, R. S. J., Gardeweg, M. C., Calder, E. S. & Matthews, S. J., 1997. Erosion by pyroclastic flows on Lascar volcano, Chile. Bull. Volcanol. 58, 557-565.

Sulpizio, R., Dellino, P., 2008. Sedimentology, depositional mechanisms and pulsating behaviour of pyroclastic density currents. In: Gottsman, J., Marti, J. (Eds.), Caldera Volcanism: Analysis,Modelling and Response. Developments in Volcanology. 10, 58-96.

Sulpizio, R., De Rosa, R. Donato, P., 2008. The influence of variable topography on the depositional behaviour of pyroclastic density currents: The examples of the Upper Pollara eruption (Salina Island, southern Italy). J. Volcanol. Geotherm. Res. 175, 367-385.

Valentine, G. A., 1987. Stratified flow in pyroclastic surges. Bull. Volcanol. 49, 616-630.

Walker, G. P. L., 1983. Ignimbrite types and ignimbrite problems. J. Volcanol. Geotherm. Res., 17, 65-88.

Williams, H., 1960. Volcanic history of the Guatemalan Highlands: California Univ Pubs Geol Sci 38, 1-87.

Wilson, C. J. N., 1980. The role of fluidisation in the emplacement of pyroclastic flows: an experimental approach. J. Volcanol. Geotherm. Res. 8, 231-249.

Wohletz, K.H., Sheridan, M.F., 1979. Model of Pyroclastic Surge. Geol. Soc. Am. Paper 180, 177-194.

Wohletz, K., Sheridan, M. F., Brown, W.K., 1989. Particle-size distributions and the sequential fragmentation tranport-theory applied to volcanic ash, J. Geophys. Res. 94, 15703-15721.

Yamamoto, T., Takarada, S., Suto, S., 1993. Pyroclastic flows from the 1991 eruption of Unzen volcano, Japan. Bull Volcanol 55, 166-175.

List of Figures:

Figure 1: (a) Plinian eruption column from the May 18, 1980 eruption of Mt St Helens. (b) and (c) Voluminous pyroclastic density currents traveling north through the breach at 14:03 and 15:48 local time, respectively. Photographs provided by the Cascade Volcano Observatory, United States Geologic Survey.

Figure 2: LiDAR maps of the Mt St Helens crater north through the pumice plain. The highlighted purple regions represent pre-existing topography and the highlighted yellow regions represent exposed debris avalanche hummock deposits (more hummock deposits are likely buried beneath the pyroclastic deposits). (a) This map points out the slope along the flanks and pumice plain and the names of the drainages. (b) Enlarged map of pumice plain showing outcrop names and locations. Some of the drainage and outcrops are not referred to in this paper. The dashed line represents the lateral extent of flow Unit V. (c) Map of flow lines for Units III and IV. Flow lines from earlier PDCs are not represented due to the lack of exposure and clear flow direction, although they likely followed the same general trends. The darker flow line represents the dominant path of the Unit III and IV PDCs.

Figure 3: General stratigraphic column for the four major PDC flow units produced during the afternoon of the May 18th, 1980 eruption of Mt St Helens. This sketch matches most closely with deposits found in the medial depositional regions of the pumice plain (5.5-6 km from source)

Figure 4: Granulometry data for all units. (a) Median phi versus distance from source. (b) Sorting versus distance from source. (c) F2 (ash <1/16 mm) versus F1 (ash < 1 mm; after Walker, 1983).

(d) Ratio of F2/F1 versus distance from source. (e) Componentry of pumice (P), lithics (L) and crystals (C) for select lithofacies from each unit.

Figure 5: AD-1 outcrop. (a) This photograph was taken from the C-drainage looking north to where the C, D and AD drainages converge. The D-4 and AD-1 outcrops are visible here, and are separated by an older fluvial terrace. Note the change from distinct basal lithic breccia at the base of Units III and IV at D-4 to distributed (and larger) blocks in AD-1. (b) Exposure of the eastern side of the AD-1 outcrop. The person is 1.5 m for scale. (c) Sketch of AD-1 with labels. The dashed lines represent apparent imbrication based on the long-axis orientation of blocks. (d) Photograph of the entire AD-1 outcrop. Notice how the flow contacts become indistinguishable toward the west.

Figure 6: These stratigraphic sections represent the major outcrops in the medial AD drainage. The median phi, sorting and F2/F1 ratios are plotted alongside the columns. Each dot in the plots represent a sample; the lines connecting the dots are inferred. The samples that fall into the stippled shaded box on the F2/F1 diagram represent fines-depleted samples; (a) AD-1, (b) AD-2b, (c) AD-3a, (d) AD-3b.

Figure 7: AD-2b outcrop photographs. Note the repetition of Unit III and the weakly stratified layers of fine ash between several of the flow units. (a) Photograph of AD-2b showing outcrop orientation relative to Mt St Helens;flank of volcano on the right (south) side of the image. Note the 6º apparent dip of the deposits. (b) Close-up of outcrop; person1.5 meters for scale.

Figure 8: (a) Photograph of the AD-3 outcrop. (b) Sketch of the AD-3 outcrop with lithofacies and features outlined and labeled. (c) Photograph of AD-3b (the north side of the outcrop). (d) Sketch of the AD-3b outcrop with lithofacies and features outlined and labeled.

Figure 9: (a) Close-up of the AD-3b outcrop. (b) Sketch of the AD-3 outcrop with lithofacies and features outlined and labeled. Notice the truncation of Unit II by the Unit III channel scour contact. Also notice the outward dipping strata and pumice lenses just to the left (south) of the channel, interpreted here as outer-channel facies. (c) Close-up of Units I, II and the scour contact between Units II and III. Person 1.5 meters for scale. (d) Close-up photograph of the channel fill breccia. Person 1.5 meters for scale.

Figure 10: Stratigraphic sections and images for medial G, F and T drainages. The median phi, sorting and F2/F1 ratios are plotted alongside the columns. Each dot in the plots represents a sample; the lines connecting the dots are inferred. The samples that fall into the stippled shaded box on the F2/F1 diagram represent fines-depleted samples. (a) G-1, (c) F-1, (d) T-2. (b) Photo of G-1 outcrop, person holding a meter stick for scale. (e) Photo of T-2 outcrop, person holding a meter stick for scale. (f) Photo of T-1 outcrop, flank of volcano in the background. (g) Enlarged photo of boxed area in (f).

Figure 11: Stratigraphic sections for distal outcrops. The median phi, sorting and F2/F1 ratios are plotted alongside the columns. Each dot in the plots represent a sample; the lines connecting the dots are inferred. The samples that fall into the stippled shaded box on the F2/F1 diagram

represent fines-depleted samples, the ones in the gray box are fines-enriched. (a) AD-4b, (b) K-1. (c) Photograph of outcrop K-1.

Figure 12: (a) and (b) Stratigraphic columns and granulometry data for outcrops C-1 and C-2, respectively. See Figure 2 for section locations. (c) Photograph of C-1; person in the blue jacket is 1.5 meters for scale. Flow direction is from right (south) to left (north). (d) and (e) Photographs of C-2. The white lines in the second photograph trace diffuse stratification; the white filled in regions are pumice lenses (lensP). The disrupted feature on the north side of the C-2 outcrop (left side of photograph d) is a small slump feature, either caused by melting ice beneath the deposits and/or a small phreatic explosion shortly after deposition.
See Table 2 for a full list of lithofacies. The key applies to all stratigraphic columns in the manuscript.

Figure 13: (a) and (d) Photograph of outcrop D-4 taken from near the AD-D convergence, looking north and upstream within the D-drainage. Flow direction in this location is N25ºW, which is (roughly) oblique but into the D-4 outcrop. (b) and (c) Close ups of the arcuate scours and lithic levees, respectively. (e) Sketch of the outcrop with labels and outlines of the imbrication and stratification within the levees. (f) Expanded sketch of levees with relative time surfaces (t) and channel fill. Time surfaces are approximate and meant to illustrate the building of the levee over time. This illustration is based on Figure 6.6E in Branney and Kokelaar (2002).

Figure 14: The analysis plotted here is for Unit IV. (a) Roundness value plotted with distance from source for the bulk pumice and grain sizes between 8-16 mm and 16-32 mm (see legend).

Note that the R-value for pumice of May 18th, 1980 MSH fall deposits is 0.78±.08 (Manga et al., 2011). (b) and (c) Frequency of roundness values comparing location F-1 (upstream from debris avalanche hummocks) with location T-1 (directly downstream from debris avalanche hummocks); see Figure 2b. Note the decrease in roundness for the 8-16 mm grain size and the bimodal distribution for the 16-32 mm clasts.

Figure 15: Location *a* and *b* in (a) represent outcrops directly downstream from hummocks where outsized blocks were noted. (b) Location *b*, 5.1 km from source. (c) Location *a* (Outcrop T-1), 7.1 km from source. A 1.5 m tall person is shown for scale in both photographs.

Figure 16: Photographs from location AD-4a, taken from west side of drainage looking towards the northeast. (a) Regional photo showing PDC deposits in relationship to debris avalanche (DA) deposits. The box is magnified in (b); (c) outline of a ~65 m wavelength, low amplitude (<7 m) mega-cross bed.

Figure 1

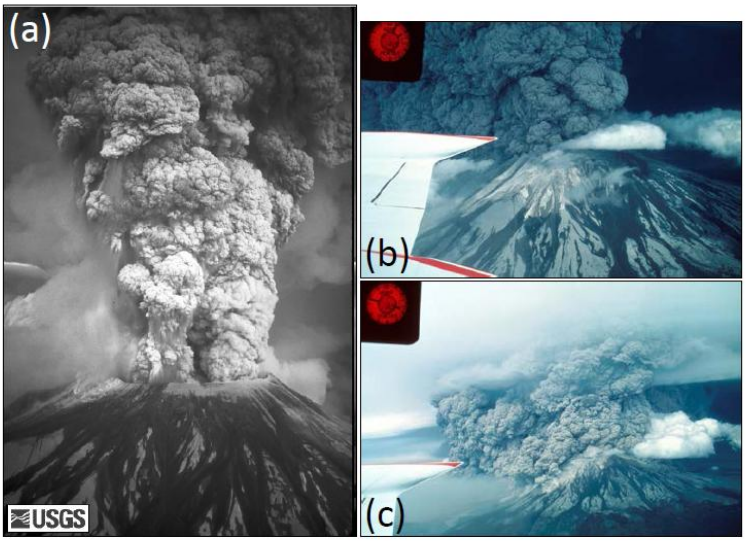

Figure 2

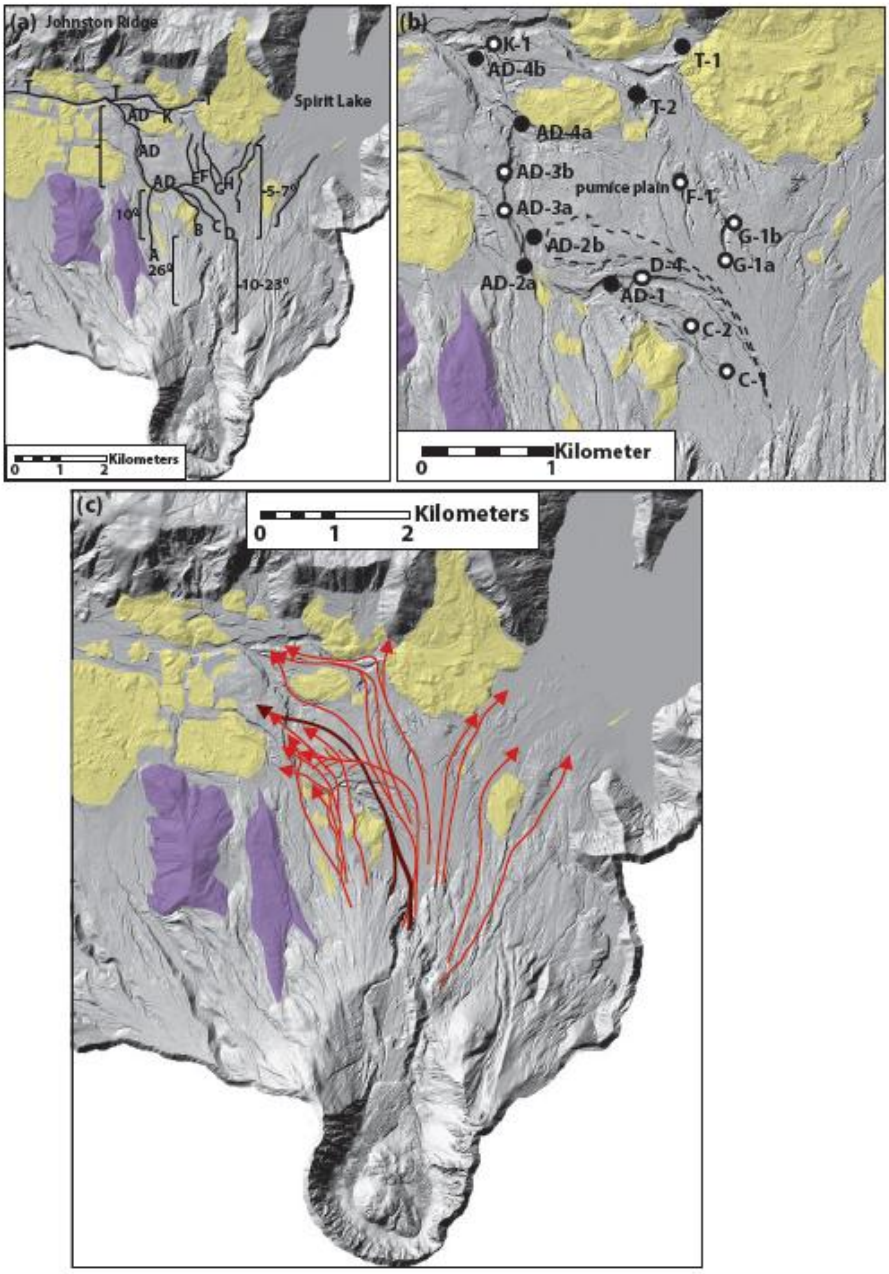

Figure 3:

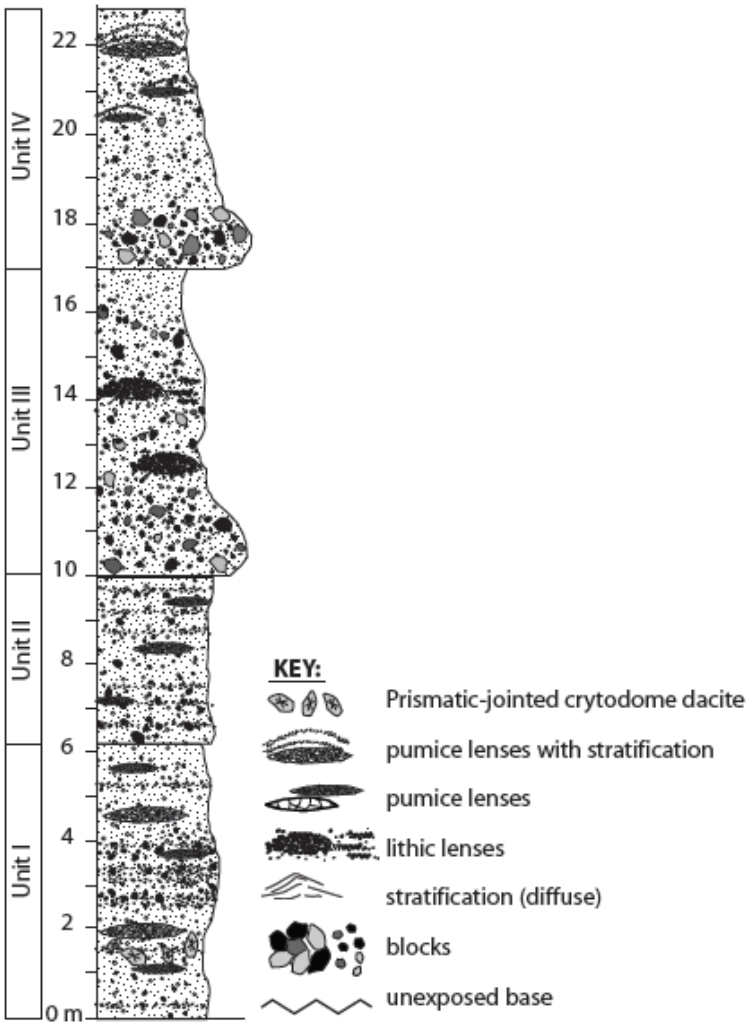

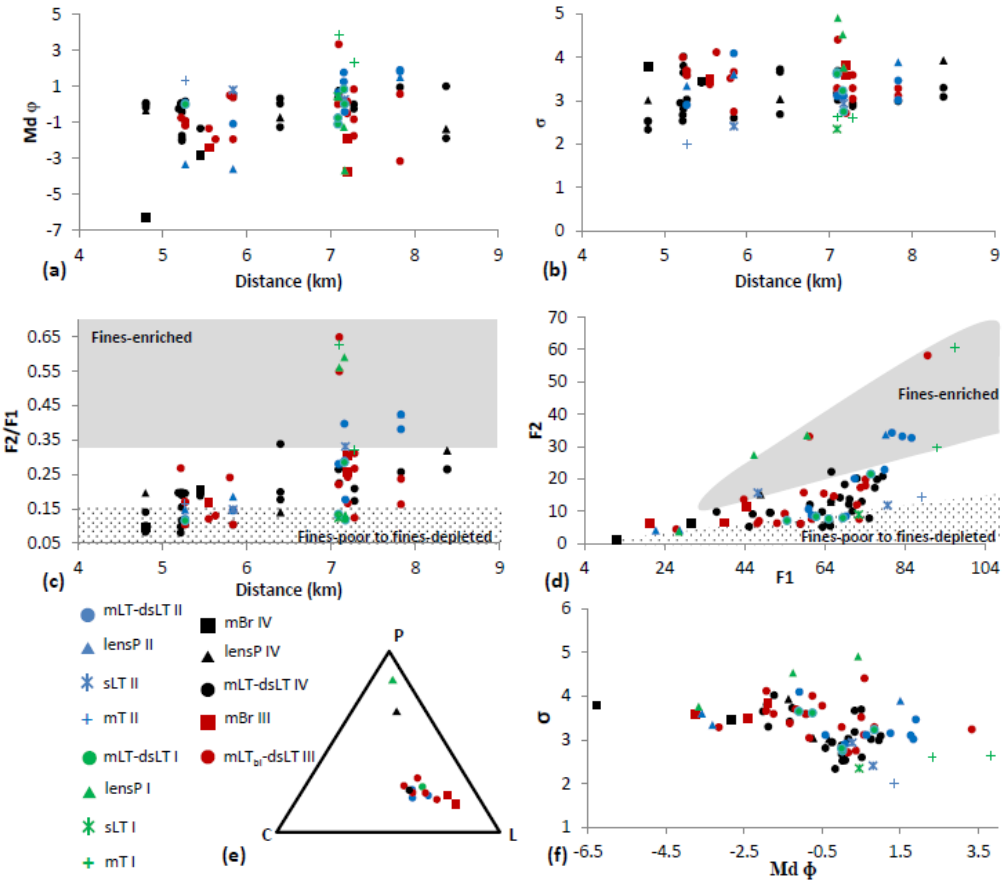

Figure 4

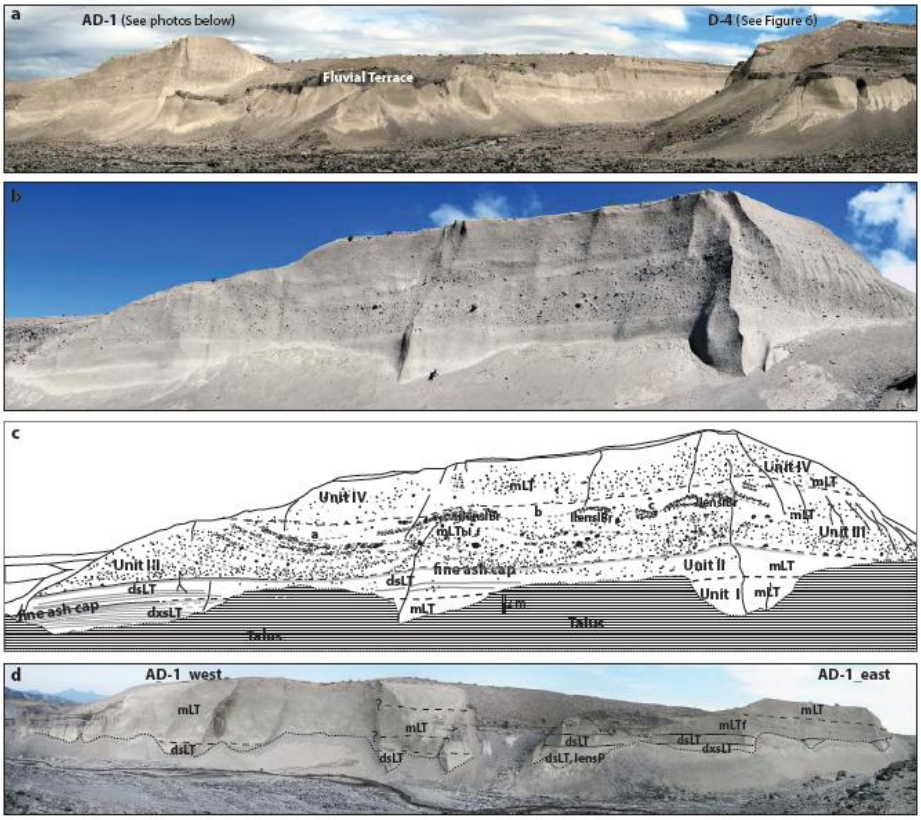

Figure 5

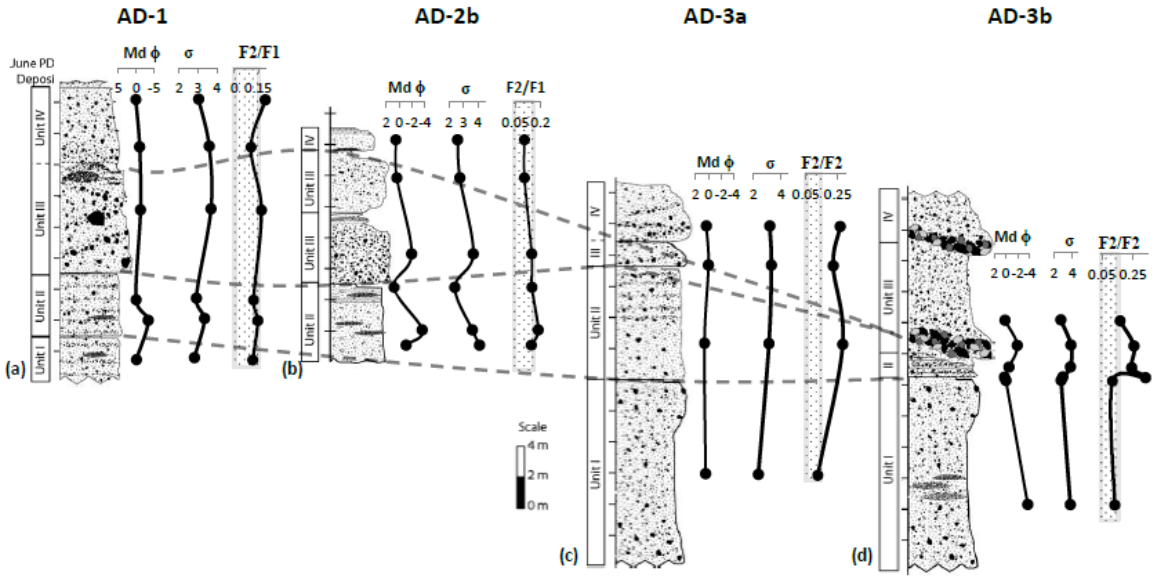

Figure 6

Figure 7

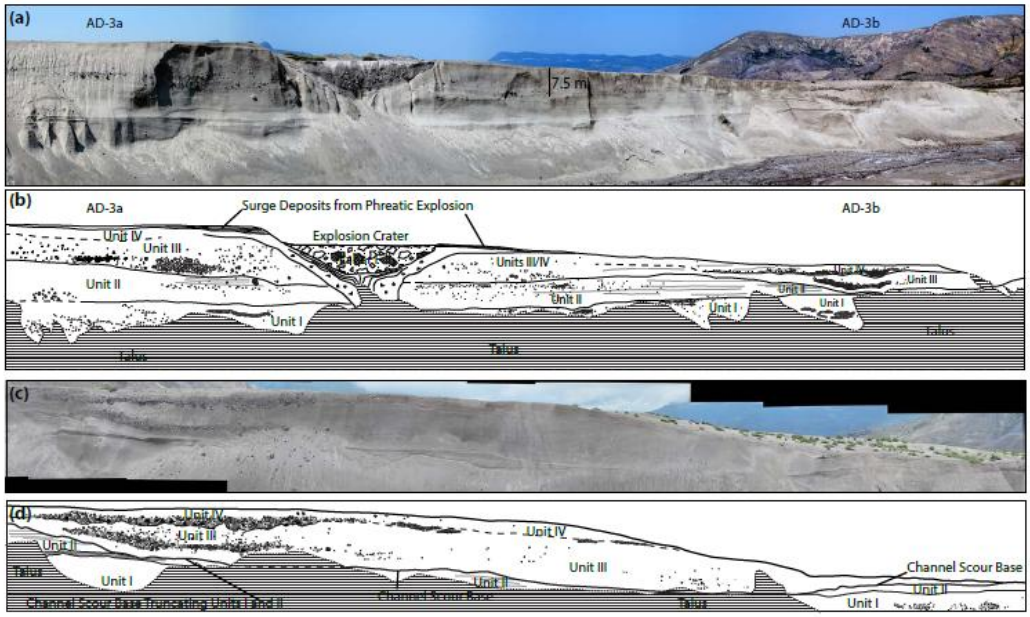

Figure 8

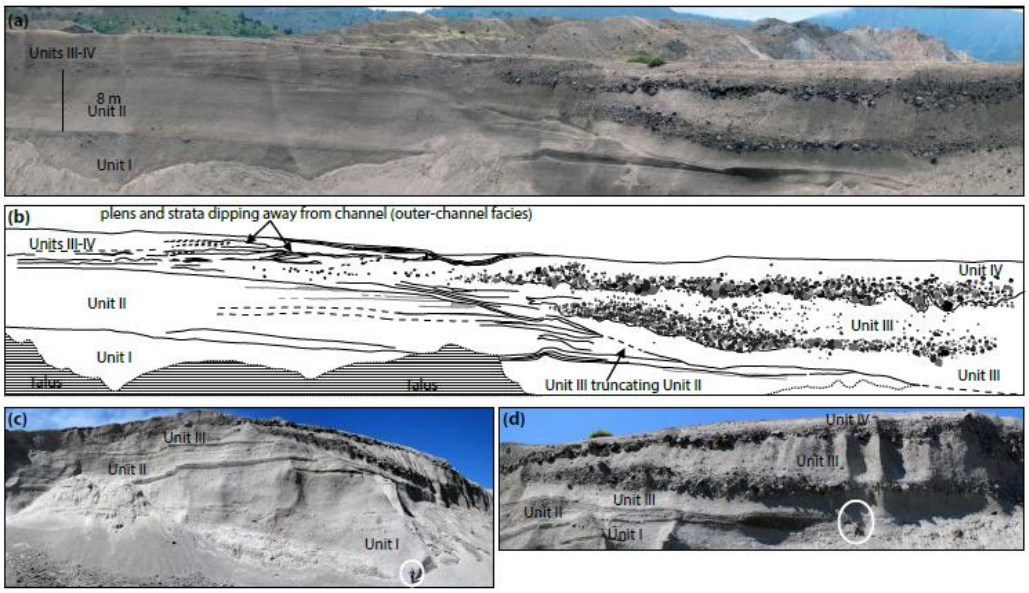

Figure 9

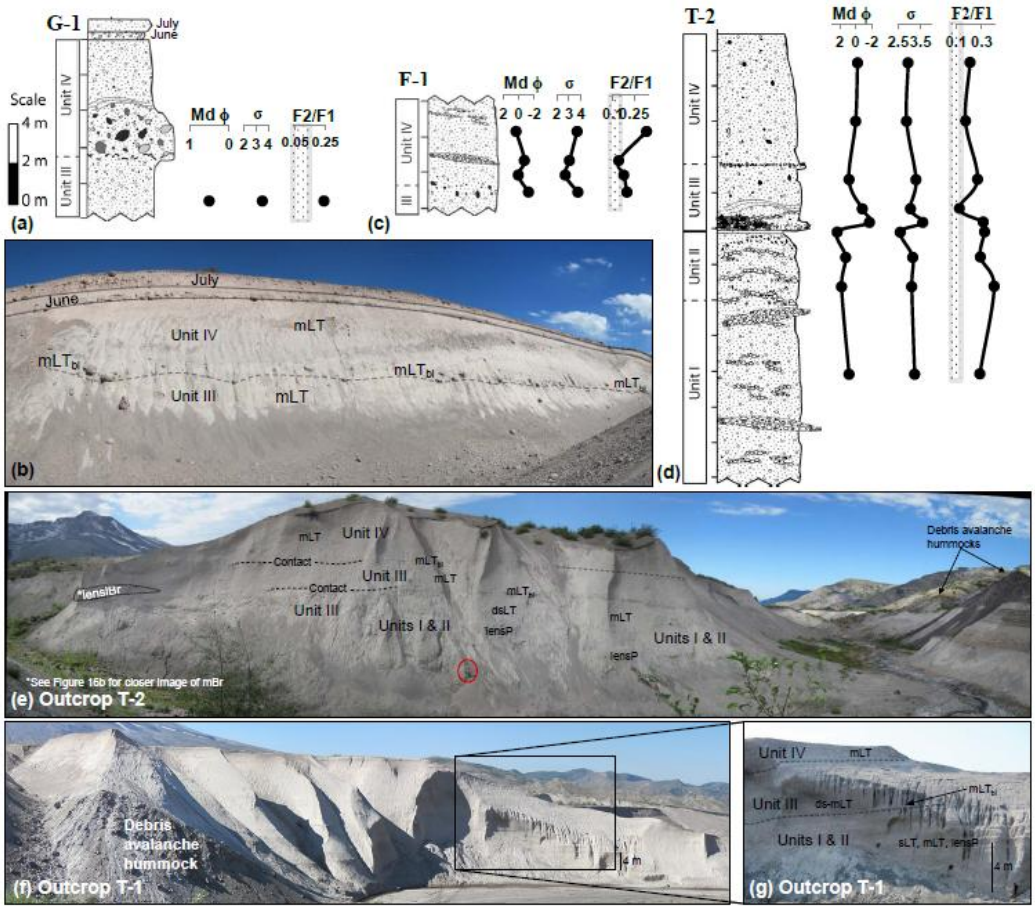

Figure 10

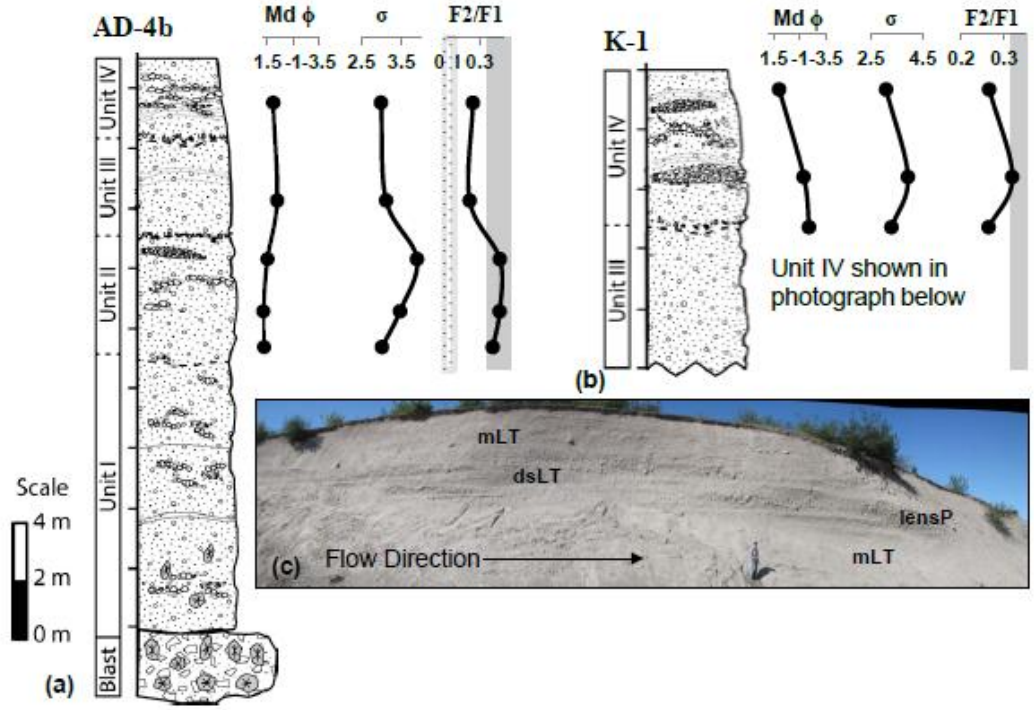

Figure 11

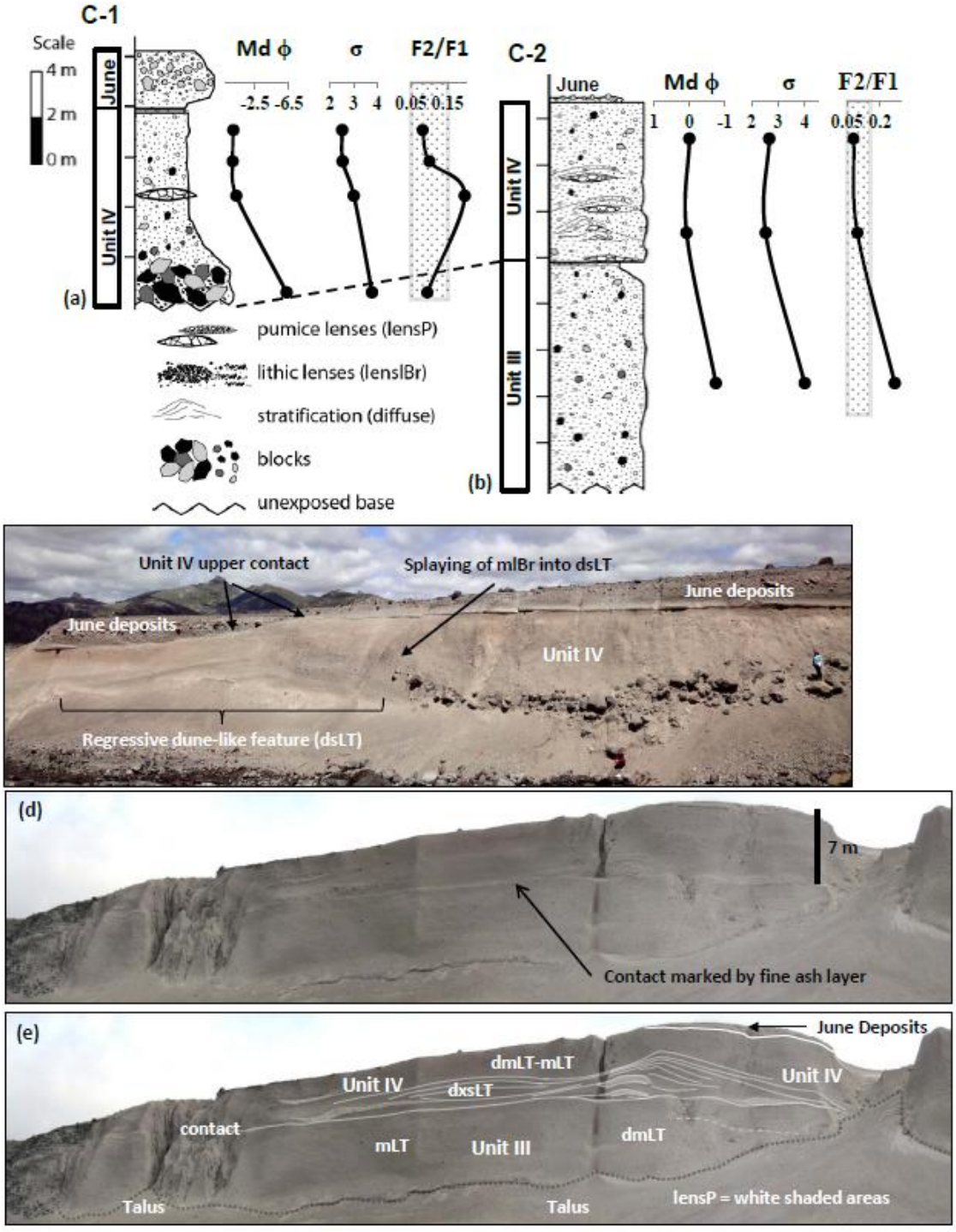

Figure 12

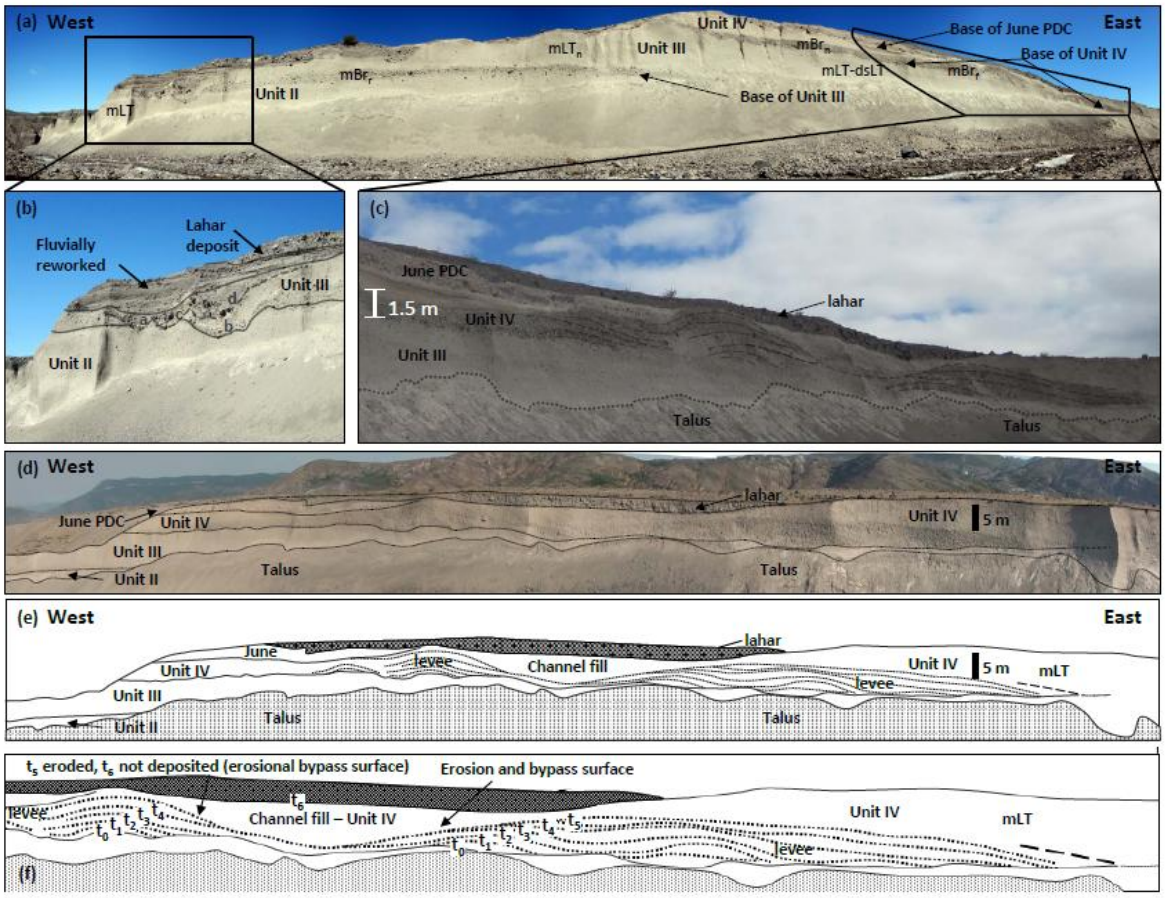

Figure 13

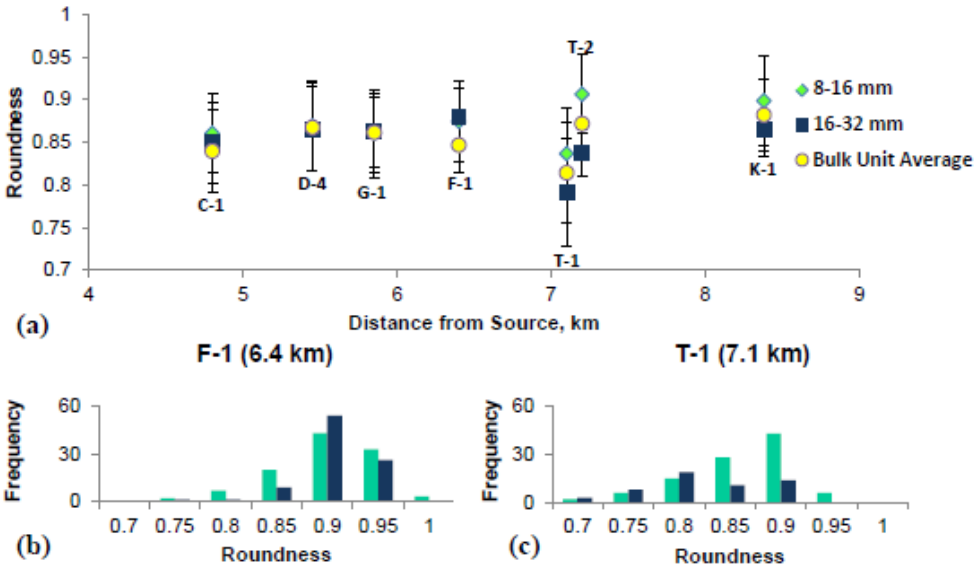

Figure 14

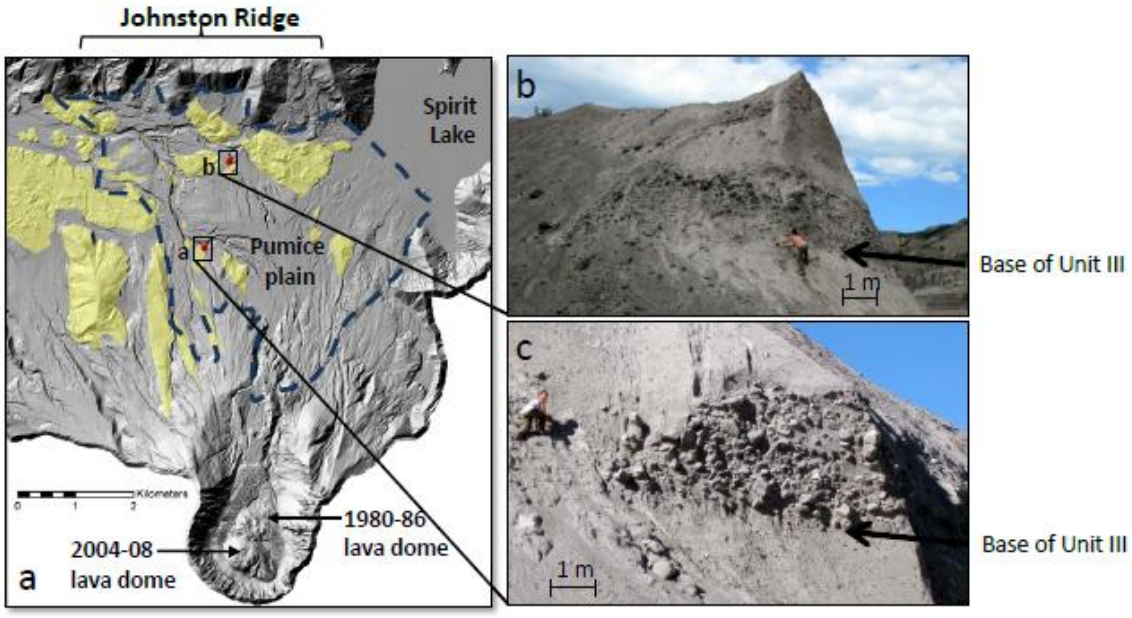

Figure 15

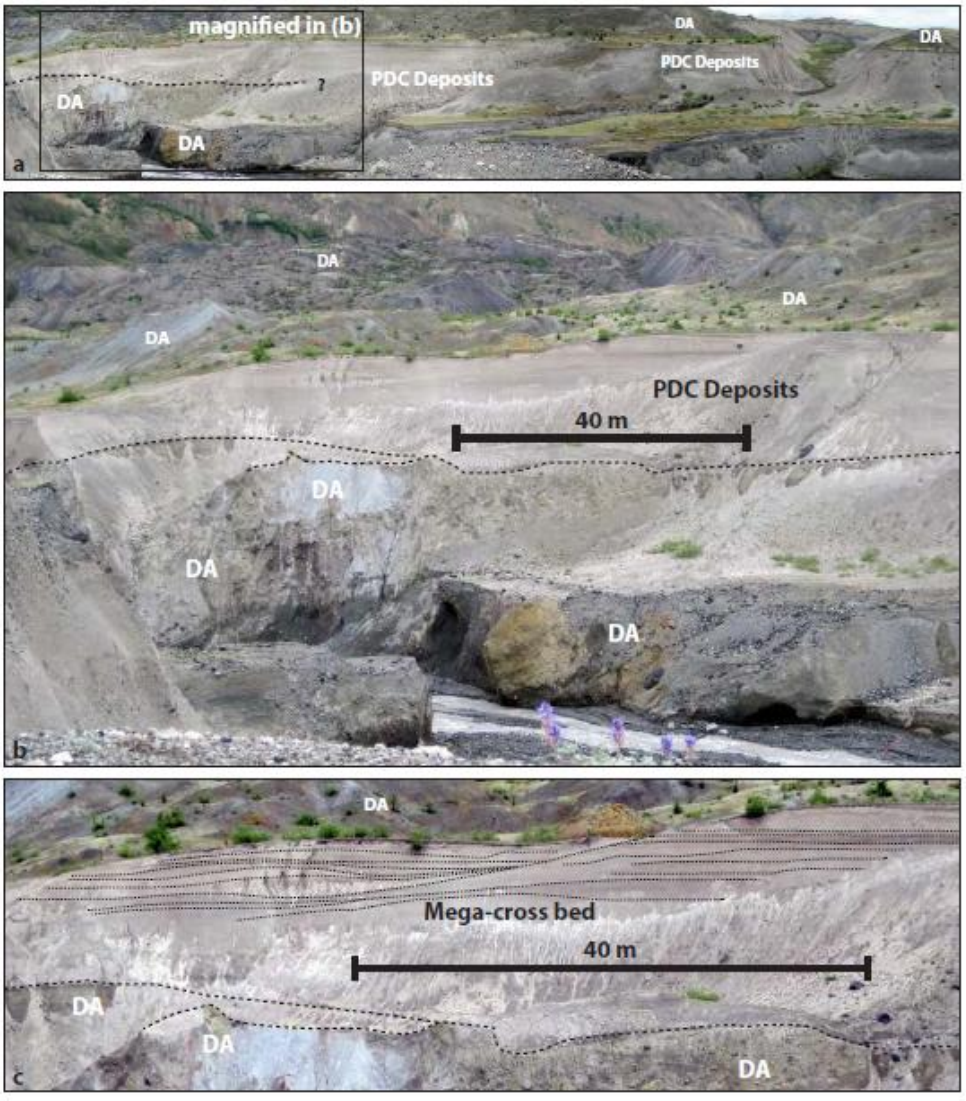

Figure 16

Table 1: Summary of phases during the May 18, 1980 eruption with relative timing and duration the PDCs that flowed down the breach (modified from Criswell, 1987). We only list the voluminous PDCs that traveled through the north breach and across the pumice plain. PDCs down the east, south and west flanks of the volcano were minor in comparison and as such are not listed here. Column height and mass flux estimates after Carey et al. (1990) and Andrews and Gardner (2009).

Phase	Time (hours)	Eruption Style	Column height; Mass flux (kg/s)	Timing and Duration of north breach funneled PDCs
I	0832-0900	Massive landslide followed by lateral blast	Not reported	Lateral blast reached maximum distance in 5-7 minutes
II	0900-1215	Early Plinian	15-18 km; $6.3x10^6$ - $1.3x10^7$ kg/s	N/A
III	1215-1500	Early Ash Flow	13-16 km; $3.9x10^6$ kg/s	1217 - PDC "poured through the breach", generating 4-7 km elongated ash cloud; 1330-1400 - episodic PDCs emplaced in the upper Toutle Valley (unclear if these reached the pumice plain); 1430-1500 size of flows increased
IV	1500-1715	Climactic phase	13-16 km; $4.0x10^7$ kg/s	1500 - "numerous, large" PDCs were observed to spill over the crater rim, engulfing the volcano, reaching spirit lake. PDC flux to the north abated around 1635. PDC activity that began to wane at 1605, ceasing at 1635.
V	1715-1815	Late Ash Flow	Not reported	Short-lived increase in activity during the waning phase produced a PDC pulse that flowed into the upper Toutle valley at 1745, reaching Spirit Lake at 1747. A second PDC pulse to the north occurred at 1810.
VI	1815-May 19^{th} 1980	Post eruption phase	N/A	N/A

Table 2:

Symbol	Lithofacies
mLT	massive lapilli tuff
mLT_f	massive lapilli tuff with fabric
mLTbl	block-rich massive lapilli tuff
mLTbl_f	massive lapilli tuff with fabric
mlBr	massive lithic breccia
sLT	stratified lapilli tuff
xsLT	cross-stratified
dsLT	diffuse stratified lapilli tuff
dxsLT	diffuse cross-stratified lapilli tuff
lensP	pumice lens
lenslBr	lithic breccia lens

Table 3: Outcrop locations, distance from source and unit thickness. Distances are approximated from the center of the crater. Text in gray indicates not fully exposed (base buried or top eroded), italicized text is estimated and "—" indicates unexposed.

Location	UTM	UTM	Distance (km)	Unit I (m)	Unit II (m)	Unit III (m)	Unit IV (m)
C-1	562715.5	5121085	4.8	--	--	--	**7.8**
C-2	562525.2	5121364	5.22	--	--	**8**	**6**
D-4	561987	5121706	5.55	--	**3**	**9**	**10**
AD-1	561906.6	5121691	5.27	**3**	**3.5**	**7**	**5**
AD-2a	561209.2	5121813	5.63	**2**	**7.5**	**6**	**5.3**
AD-2b	561238.8	5122078	5.84	**5.8**	**5.7**	**9.5**	**3**
AD-3a	561007	5122249	7.09	**10**	**8**	**5**	**2.8**
AD-3b	560984.9	5122402	7.17	**12**	**8**	**8**	**3**
AD-3c	560999.8	5122477	7.19	--	**4.33**	**8**	**3**
AD-4b	560833.1	5123276	7.83	**8.9**	**4**	**3.5**	**2.5**
K-1	560922	5123421	8.38	--	--	**4.5**	**5.7**
G-1a-b	562673	5122035	5.8	--	--	**4.5**	**5.6**
F-1	562299	5122507	6.4	--	--	--	**6**
T-1	562314.6	5123490	7.1	**7**	**3.8**	**5**	**5.5**
T-2	562014.6	5123171	7.16	**10**	**4**	**3.9**	**7.7**

Table 4: General introduction, description and interpretation of major flow Units.

	General Description	General Interpretation
Unit I	Unit 1 contains a variety of lithofacies including diffusely- stratified lapilli tuff (dsLT), diffusely cross-stratified lapilli tuff (dxsLT), massive lapilli tuff (mLT), block-rich massive lapilli tuff (mLT_{bl}) and pumice lenses (lensP; Table 2). The diffuse stratification is a result of subtle grain size variations at centimeter to decimeter intervals. Unit I is often capped with a thin (<50 cm) layer of fine-grained, massive ash (mT).	Massive PDC deposits with no apparent fabric, such as mLT, are often interpreted to be the result of rapid deposition from a concentrated basal region of the flow where shear stresses are negligible (e.g., Branney and Kokelaar, 2002). Stratification, such that occurs in lithofacies dsLT and dxsLT, is associated with traction-dominated flow boundary conditions occurring from higher basal shear stress conditions relative to those that produce mLT. The lateral gradation between dsLT, dxsLT and mLT over short spatial distances within Units I and II attest to the unsteady and non-uniform conditions in the depositional system of the current.
Unit II	Unit II is gradational between the mLT and dsLT lithofacies. Stratification occurs on the scale of centimeters to decimeters, thickens and thins laterally, and appears to be the consequence of subtle variations in grain size. Where massive, the unit often displays normal grading from the base to the middle and reverse grading within the uppermost 1-2 m. Well-stratified lapilli tuff (sLT) occurs rarely and only locally. Pumice lenses (lensP) are common and increase in abundance, size and grain size with distance from source (Figure 4a). Unit II is locally capped by a 20-50 cm thick layer of fine-grained, massive ash.	
Unit III	Unit III, on average the thickest and most poorly-sorted of the five major flow units, is a massive, block-rich lapilli tuff (mLT_{bl}). The blocks can be (1) concentrated in a basal breccia for 10s of meters laterally (mlBr), (2) concentrated in lenticular, convex-shaped pods (lenslBr) of variable size (most commonly 1-3 m across, but up to 10s of meters) throughout the flow unit, or (3) randomly dispersed throughout the flow unit with weak grain fabric ($mLT_{bl\,f}$) (Figure 3). The lithic concentrations grade vertically and laterally into mLT**bl** with infrequent diffuse bedding structures and weak grain fabric. Pumice lenses are not present. Rarely a fine-ash layer can be found capping Unit III.	The general lack of fines depletion, absence of lensP, and the more general distribution of lithic blocks throughout Unit III rather than development of a widespread lithic rich base suggests that the current was at the high end of concentrated flow, resulting in strongly suppressed density segregation and elutriation across the entire depositional area (45-65 vol% particles; Selim et al., 1983; Druitt, 1995). The massive nature of the deposits suggests high internal pore pressure was the dominant particle support mechanism within the depositional region over the duration of flow and deposition (e.g., Roche, 2012). The commonly erosive nature of the Unit II-III contact also suggests that the Unit III current had a strong erosive capacity.

Unit IV	The base of Unit IV is often denoted by mlBr, which grades vertically into poorly-sorted, mostly structureless mLT. The most proximal lithic breccia at the base of Unit IV is the coarsest lithic breccia out of all five flow units (Figure 5); however, the size and abundance of lithic blocks decreases abruptly downstream. The mLT is primarily fines-depleted up to 6 km from source. Beyond 6 km the mLT varies widely from fines-poor to fines-normal across the expanse of the depositional area with no discernible trends with distance from source or between lithofacies (Figure 4c, d). Coarse lapilli lensP are common at all locations, but increase in abundance, grain size and size with distance from source.	The massive nature of Unit IV and lack of obvious fabric suggests deposition from a concentrated current with rapid sedimentation and low basal shear stress (e.g., Branney and Kokelaar, 2002). However, the block-rich nature of the base and presence of well- developed lensP suggests density segregation was more efficient compared to Unit III. A transition from fines poor deposits in proximal-medical locations to fines normal deposits from medial-distal locations suggests sedimentation fluidization within the depositional region was important during the first half of the transport distance, but transitioned to a current dominated by high internal pore pressure in the second half of the travel distance, likely due to a decrease in pore space as the flow compacted.
Unit V	Unit V is a spatially-limited, pumice-rich, poorly-sorted mLT. It extends locally across the surface of the pumice plain up to 6.5 km from source, but is only exposed in cross section in the proximal sections of the D-drainage within 5.25 km from source (dashed line in Figure 2b). The surface of Unit V is a perfect example of primary, meandering, cross-cutting and onlapping pumice lobes and levees, which can be found along the surface just north of the D-drainage (Figure 2). The lowermost portion of the unit extends the furthest across the pumice plain, and the onlapping pumice lobes are deposited more proximal to source in a back-stepping fashion. Unit V is a minor, local unit with poor exposures; as such it is not discussed further in this paper.	Unit V deposits are massive and lack fabric, suggesting deposition from a concentrated current with rapid sedimentation rates and low basal shear stress (e.g., Branney and Kokelaar, 2002). The pumice-rich lobes and levees are characteristic surface features of pumice flows (e.g., Calder et al., 2000; Pittari et al., 2005; Jessop et al, 2012). We interpret that the pumice segregated and was transported to the outside of the current, where the larger pumice clasts became concentrated along the deposit margins or flow fronts (e.g., Sparks, 1976; Calder et al., 2000; Pittari et al., 2005). The back-stepping of the onlapping pumice lobes suggests deposition from a waning current.

Research Highlights:

- Self-channelization increases pyroclastic current capacity and runout distance.
- Substrate erosion occurs at the head and within the body of a pyroclastic current.
- Substrate erosion is enhanced by surface roughness.
- Internal pore pressure is a primary particle support mechanism.
- Internal pore pressure never completely diffuses across the depositional region.